PHILOSOPHICAL TRANSACTIONS OF THE ROYAL SOCIETY B BIOLOGICAL SCIENCES

The Aerodynamics of Hovering Insect Flight. VI. Lift and Power Requirements

C. P. Ellington

Phil. Trans. R. Soc. Lond. B 1984 **305**, 145-181
doi: 10.1098/rstb.1984.0054

Phil. Trans. R. Soc. Lond. B **305**, 145–181 (1984) [145]
Printed in Great Britain

THE AERODYNAMICS OF HOVERING INSECT FLIGHT. VI. LIFT AND POWER REQUIREMENTS

BY C. P. ELLINGTON
Department of Zoology, University of Cambridge, Downing Street, Cambridge CB2 3EJ, U.K.

(*Communicated by Sir James Lighthill, F.R.S.* – *Received* 28 *March* 1983)

CONTENTS

The lift and power requirements for hovering insect flight are estimated by combining the morphological and kinematic data from papers II and III with the aerodynamic analyses of papers IV and V. The lift calculations are used to evaluate the importance in hovering of two distinct types of aerodynamic mechanisms: (i) the usual quasi-steady mechanism, where the circulation for lift is primarily determined by translation of the wing, and (ii) rotational mechanisms, where the circulation is largely governed by wing rotation at either end of the wingbeat. Power estimates are compared with the available measurements of metabolic rate during hovering to investigate the role of elastic energy storage, the maximum mechanical power output of the flight muscles, and the muscle efficiency.

The quasi-steady mechanism proves inadequate for the lift requirements of hover-flies using an inclined stroke plane, and for a ladybird beetle and a crane-fly hovering with a horizontal stroke plane. Observed angles of attack rule out lift enhancement by unsteady modifications to the quasi-steady mechanism, such as delayed stall, but the rotational lift mechanisms proposed in paper IV seem consistent with the kinematics. The rotational mechanisms rely on concentrated vortex shedding from the leading edge during rotation, with attachment of that vorticity as a leading edge separation bubble during the subsequent half-stroke. Strong leading edge vortex shedding should result from delayed pronation for the hover-fly, a near fling and partial fling for the ladybird, and profile flexion for the crane-fly (the flex mechanism).

The kinematics for the other insects hovering with a horizontal stroke plane are basically the same as for the anomalous crane-fly, and the quasi-steady mechanism cannot be accepted for them while rejecting it for the crane-fly. All of these insects flex their wings in a similar manner during rotation, and could use the flex mechanism for lift generation. The implication is that most, if not all, hovering animals do not rely on quasi-steady aerodynamics, but use rotational lift mechanisms instead.

It is not possible to reconcile the power estimates with the commonly accepted values of both the mechanochemical efficiency of insect flight muscle (about 25 %) and its maximum mechanical power output (about 20 W N^{-1} of muscle). Maximum efficiencies of 12–29 % could be obtained only if there is no elastic storage of the kinetic energy of the flapping wings, but this would require more than twice the accepted value for maximum mechanical power output. The available evidence suggests that substantial elastic storage does occur, and that the maximum mechanical power output is close to the accepted value. If so, then the efficiency of both fibrillar and non-fibrillar flight muscle is likely to be only 5–9 %.

1. Introduction

The preceding papers of this study considered four more or less separable aspects of the aerodynamics of hovering insect flight: morphology, kinematics, lift mechanisms and aerodynamic theory. In this final paper, these aspects are brought together to estimate the lift and power requirements for the insects from the film sequences selected in paper III. Equations for lift and power are derived for animals with only one pair of 'wings' in an aerodynamic sense: the equations are difficult enough without introducing the complications of uncoupled fore- and hind-wings, as would have been necessary if hovering film sequences had been obtained for *Chrysopa carnea*. Morphological and kinematic data from papers II and III are then used in the equations to calculate numerical estimates.

To simplify the analysis it will be assumed that the duration of the downstroke is equal to the upstroke, and that the wing motion is confined to the stroke plane. These helpful assumptions are not necessary, but judging by the results of paper III they will introduce no

significant errors. The relative stroke plane defined in paper V will be used in calculating the aerodynamic forces with respect to the relative velocity of the wings; this approximation effectively reduces a three dimensional problem to a two dimensional one, and gives but small errors in the direction and magnitude of the force vectors. Bars and 'hats' over symbols will denote mean and non-dimensional values as before. In case the reader has forgotten the meaning of any symbols used in the earlier papers, the symbol table in paper I should prove useful.

2. Equations for lift

2.1. *Relative stroke plane angle*

The relative velocity of the wing, equal to the vector sum of the flapping velocity U and the induced velocity w_0, is an important determinant of the aerodynamic forces. The relative velocity is approximately parallel to the relative stroke plane, and its magnitude U_r can be estimated from equation (V. 8) as

$$U_r = U\cos\beta/\cos\beta_r. \tag{1}$$

(Equations from other papers in this series will be identified by the paper number in roman numerals, followed by the equation number within that paper; e.g., equation (V. 8) refers to equation (8) of paper V.) The lift and profile drag forces are perpendicular and parallel to the relative velocity, respectively, and hence are perpendicular and parallel to the relative stroke plane for each half-stroke. The angle β_r between the relative stroke plane and the horizontal must therefore be determined before the aerodynamic forces can be investigated. This angle differs for the half-strokes, and it is given by equation (V. 46) as

$$\tan\beta_r = \tan\beta \pm \frac{P^*_{RF}(1+\tau)}{2\Phi nR\cos\beta}, \tag{2}$$

where the negative sign applies to the downstroke and the positive to the upstroke, and the stroke angle Φ is in radians. The second term on the right-hand side is equal to the mean induced velocity during the lift impulse divided by the horizontal component of the mean wing tip velocity. This term can also be expressed using the spacing parameter s from equation (V. 36) if s is written as

$$s^2 = \frac{8\pi p_w}{\rho \hat{f}^2 n^2 \Phi^2 R^2 \mathcal{R}\cos^2\beta}, \tag{3}$$

where p_w is the wing loading. The non-dimensional frequency $\hat{f}$ equals the vertical impulse frequency f divided by the wingbeat frequency n; the value of $\hat{f}$ is 2 if both half-strokes provide weight support, and 1 if only one does so. Equation (2) can then be transformed into

$$\tan\beta_r = \tan\beta \pm \frac{\hat{f}s(1+0.079\,s^2)}{4\sqrt{(\pi\Phi\cos\beta)}}. \tag{4}$$

We now consider the aerodynamic mechanisms that might produce the lift required for hovering flight. Many mechanisms were propounded in paper IV, but it is not necessary, or not possible in some cases, to investigate them individually. In fact, it will be sufficient to examine only two broad categories: (i) the quasi-steady mechanism, where the circulation around a wing element is primarily determined by translation of the wing, and (ii) rotational mechanisms, where the circulation is largely governed by wing rotation.

PHILOSOPHICAL TRANSACTIONS OF THE ROYAL SOCIETY B BIOLOGICAL SCIENCES

2.2. *Quasi-steady mechanism*

The quasi-steady mechanism assumes that the lift force on a flapping wing is equal to that experienced in steady motion at the same instantaneous linear velocity and attitude. The validity of this assumption for hovering animal flight has been tested by several authors using the proof-by-contradiction outlined in paper I (Weis-Fogh 1972, 1973; Ellington 1975; R. Å. Norberg 1975; U. M. Norberg 1975, 1976). Following Osborne (1951), a mean value of the lift coefficient $\overline{C_L}$ is found that satisfies the mean lift requirement. This is equivalent to assuming that the effective angle of incidence, and hence the lift coefficient C_L, is constant along the wing and throughout the cycle. According to the kinematic results of paper III, this assumption is reasonable as long as the rotational phases at either end of the wingbeat are ignored. Neglect of the rotational phases is consistent with the quasi-steady mechanism, though, because the low translational velocities during rotation would produce very little lift. The mean lift coefficient obtained in this manner is particularly informative because it is the minimum value of C_L compatible with flight: if C_L varies during the wingbeat, then some instantaneous values must exceed the mean, $\overline{C_L}$.

The mean lift coefficient will be derived from the impulse method of the vortex theory in paper V, but it can also be found from the usual blade-element equations as outlined in paper I. Assuming C_L is equal to the mean value $\overline{C_L}$, the circulation around each wing element is given by

$$\Gamma = \tfrac{1}{2} c U_r \overline{C_L}. \tag{5}$$

Equation (1) and the definition of the flapping velocity $U = r(\mathrm{d}\phi/\mathrm{d}t)$ can be substituted into equation (5), which can then be expressed in terms of the non-dimensional parameters of papers II and III;

$$\Gamma = \frac{n\Phi S \cos\beta}{8\cos\beta_r} \overline{C_L}\, \hat{c}\hat{r}(\mathrm{d}\hat{\phi}/\mathrm{d}\hat{t}); \tag{6}$$

the total wing area S should not be confused with the spacing parameter s. The maximum circulation Γ_{max} occurs when both $\mathrm{d}\hat{\phi}/\mathrm{d}\hat{t}$ and the product $\hat{c}\hat{r}$ are maxima. The non-dimensional circulation $\hat{\Gamma}$ $(= \Gamma/\Gamma_{max})$ is therefore

$$\hat{\Gamma} = \frac{\hat{c}\hat{r}(\mathrm{d}\hat{\phi}/\mathrm{d}\hat{t})}{(\hat{c}\hat{r})_{max}(\mathrm{d}\hat{\phi}/\mathrm{d}\hat{t})_{max}}. \tag{7}$$

Equation (7) can be substituted into equation (V. 5) to find the non-dimensional impulse $\hat{I}$ from circulatory lift over a half-stroke. The resulting expression for $\hat{I}$ is based on the assumption of a constant lift coefficient equal to $\overline{C_L}$, and it will be written as $\hat{I}(\overline{C_L})$ in recognition of this:

$$\hat{I}(\overline{C_L}) = \frac{1}{(\hat{c}\hat{r})_{max}(\mathrm{d}\hat{\phi}/\mathrm{d}\hat{t})_{max}} \int_{-1}^{1} \frac{\mathrm{d}\hat{\phi}}{\mathrm{d}\hat{t}}\,\mathrm{d}\hat{\phi} \int_0^1 \hat{c}\hat{r}^2\,\mathrm{d}\hat{r}. \tag{8}$$

The integral with respect to $\mathrm{d}\hat{r}$ is simply the non-dimensional second moment of wing area from paper II, $\hat{r}_2^2(S)$. The other integral equals $\frac{1}{2}$ times the mean square of $\mathrm{d}\hat{\phi}/\mathrm{d}\hat{t}$, which is given in paper III. Thus the non-dimensional impulse is

$$\hat{I}(\overline{C_L}) = \frac{\hat{r}_2^2(S)\,\overline{(\mathrm{d}\hat{\phi}/\mathrm{d}\hat{t})^2}}{2(\hat{c}\hat{r})_{max}(\mathrm{d}\hat{\phi}/\mathrm{d}\hat{t})_{max}}. \tag{9}$$

The mean lift $\overline{L}$ over a half-stroke was given in paper V as $2nI$, where I is the impulse of the vortex sheet created by circulatory lift: from equation (V. 5) and the definition of A_r,

$$\overline{L} = 2\rho n \Phi R^2 \Gamma_{max} \hat{I} \cos\beta/\cos\beta_r. \tag{10}$$

Substitution of equations (6) and (9) yields

$$\overline{L} = \frac{\rho n^2 \Phi^2 R^2 S \hat{r}_2^2(S) \overline{(d\hat{\phi}/d\hat{t})^2} \cos^2\beta}{8\cos^2\beta_r} \overline{C_L}. \tag{11}$$

We can define a non-dimensional mean lift $\overline{\hat{L}}$ over the half-stroke equal to $\overline{L}$ divided by mg, and solve for the mean lift coefficient in terms of the wing loading p_w $(=mg/S)$,

$$\overline{C_L} = \frac{8 p_w \overline{\hat{L}} \cos^2\beta_r}{\rho n^2 \Phi^2 R^2 \hat{r}_2^2(S) \overline{(d\hat{\phi}/d\hat{t})^2} \cos^2\beta}. \tag{12}$$

No assumptions about the direction and magnitude of the mean lift force have been invoked in this derivation of $\overline{C_L}$, so equation (12) may be used to calculate the mean lift coefficient required by the quasi-steady mechanism to produce a mean lift force of $mg\overline{\hat{L}}$ during any half-stroke in hovering flight; this mean lift force is not necessarily vertical.

We now return to the problem of aerodynamic mechanisms after that brief mathematical interlude. Apart from wing rotation, there are two effects which are not included in the quasi-steady mechanism: the *Wagner effect*, and the *delayed stall* of translation (paper IV). In the Wagner effect, the instantaneous circulation around a wing element lags behind the quasi-steady value because of the induced velocity field of shed vorticity. The 'starting' vorticity shed at the beginning of a half-stroke will therefore delay the growth of circulation around the wings. The induced velocity field of the 'starting' vorticity will also be augmented by that of any 'stopping' vorticity from the preceding half-stroke, so the growth of circulation can be delayed even more than usual. Because the wings move but a few chord lengths, the circulation is unlikely to reach its full value before beginning to decay towards the end of the half-stroke. Thus the predicted maximum circulation Γ_{max} will not be realized, and the mean lift over the half-stroke will be reduced. The extent of this effect cannot be estimated, however; the Wagner effect has only been analysed for two-dimensional aerofoils, and the results should not be applied directly to the three-dimensional pattern of shed vorticity in hovering. All that can be done at present is to appreciate that substantially more lift will be required of the wings than is indicated by $\overline{C_L}$ from the quasi-steady assumption.

The delayed stall of translation allows a wing to operate effectively above the stall angle for a few chords of translation. For a brief period, the wings can therefore generate more lift than would be expected under quasi-steady conditions. The effective angles of incidence during hovering will be estimated later to determine whether or not animals do rely on delayed stall. If they do, then the growth of the enhanced circulation is still subject to the Wagner effect (Francis & Cohen 1933).

2.3. *Rotational mechanisms*

The rotational mechanisms of paper IV offer a complete contrast to the quasi-steady mechanism and Wagner effect. Strong vortex shedding must be produced by the high angular velocity ω of rotation during pronation and supination, and it may result in a net circulation around the wings. This would generate circulation *before* translation, in contrast to its gradual

growth under the influence of the Wagner effect. The amount of circulation that can be created should be proportional to ωc^2 for *all* of the rotational mechanisms: the fling (or peel), the partial fling, the near fling, and isolated rotation (the flex mechanism). The mean angular velocity $\bar{\omega}$ during pronation and supination (paper III) can be used to define the rotational circulation around a wing element as

$$\Gamma = \gamma \bar{\omega} c^2, \tag{13}$$

where the effectiveness of the different rotational mechanisms in producing circulation will be reflected in the proportionality constant γ, which may be intrepreted as a *rotational lift coefficient*. It was argued in paper IV that several factors might help the circulation generated by the rotational mechanisms to persist during the subsequent translation of the wings: (i) the delayed stall of translation, (ii) the delayed stall of rotation, Kramer's effect, (iii) the extra circulation needed for wing rotation under the general formulation of the quasi-steady assumption, and (iv) stabilization of the leading edge bubble by spanwise transport of vorticity (Maxworthy 1979). Thus the circulation around a wing element could be almost independent of the positional angle ϕ during a half-stroke, and approximately given by equation (13).

The value of γ may vary along the wing length according to the separation distance between the elements of the wing pair during rotation. It will be assumed to be constant and equal to a mean value $\bar{\gamma}$, though, by analogy with the mean lift coefficient. The circulation of equation (13) can then be expressed in terms of the non-dimensional parameters as

$$\Gamma = \bar{\gamma} \hat{\omega} n S \hat{c}^2 / \mathcal{R}, \tag{14}$$

where $\hat{\omega}$ is the non-dimensional form of the mean angular velocity ($= \bar{\omega}/n$, from paper III). The maximum circulation occurs at the maximum chord ($\hat{c} = \hat{c}_{\max}$), thus the non-dimensional circulation is

$$\hat{\Gamma} = \hat{c}^2 / \hat{c}^2_{\max}. \tag{15}$$

$\hat{I}(\bar{\gamma})$ is equal to

$$\hat{I}(\bar{\gamma}) = \frac{1}{\hat{c}^2_{\max}} \int_{-1}^{1} \mathrm{d}\hat{\phi} \int_{0}^{1} \hat{c}^2 \hat{r} \, \mathrm{d}\hat{r} = \frac{2\hat{v}\hat{r}_1(v)}{\hat{c}^2_{\max}}, \tag{16}$$

where $\hat{v}$ is the non-dimensional virtual mass of the wing, and $\hat{r}_1(v)$ is the non-dimensional first moment of that mass (paper II). The mean lift is given by equation (10), and substitution of $\Gamma_{\max}$ and $\hat{I}(\bar{\gamma})$ yields

$$\bar{L} = 4\rho\bar{\gamma}\hat{\omega}n^2\Phi S R^2 \hat{v}\hat{r}_1(v) \cos\beta / \mathcal{R} \cos\beta_{\mathrm{r}}. \tag{17}$$

By using the definition of $\bar{L}$, we then solve for $\bar{\gamma}$ to produce the required mean lift over the half-stroke:

$$\bar{\gamma} = \frac{p_{\mathrm{w}} \bar{L} \mathcal{R} \cos\beta_{\mathrm{r}}}{4\rho\hat{\omega}n^2\Phi R^2 \hat{v}\hat{r}_1(v) \cos\beta}. \tag{18}$$

The mean lift demanded of the rotational mechanisms must be the same as that calculated for the quasi-steady mechanism, so $\bar{\gamma}$ can also be expressed as a function of the mean lift coefficient:

$$\bar{\gamma} = \frac{\Phi \mathcal{R} \hat{r}_2^2(S) \overline{(\mathrm{d}\hat{\phi}/\mathrm{d}\hat{t})^2} \cos\beta}{32\hat{\omega}\hat{v}\hat{r}_1(v) \cos\beta_{\mathrm{r}}} \overline{C_{\mathrm{L}}}. \tag{19}$$

The parameter $\bar{\gamma}$ is to the rotational mechanisms what $\overline{C_{\mathrm{L}}}$ is to the quasi-steady mechanism. Just as the estimates of $\overline{C_{\mathrm{L}}}$ will be compared with expected values to evaluate the feasibility of the quasi-steady mechanism for hovering flight, the estimates of $\bar{\gamma}$ will be tested against expectations for the rotational mechanisms. The value of $\bar{\gamma}$ admittedly conveys no intuitive 'feel'

for the amount of lift produced by the wings, however, as does the traditional lift coefficient. Because of this it is probably informative to calculate $\overline{C_L}$ even if the quasi-steady mechanism clearly does not apply to a particular type of hovering, such as a clap and fling at either end of the wingbeat.

3. Equations for power

The mechanical power requirements of flapping animal flight are traditionally divided into four components, but it is widely assumed that one of these is negligible for hovering flight. Because the flight velocity is zero in hovering, there should be no drag force on the body and therefore no power expenditure against such a force; this power component is called the *parasite power* P_{par} because the body drag is an unwelcome 'parasite' in the net force balance. The strong induced velocity field in hovering may produce a downward drag force on the body, though, which requires greater lift from the wings and thus incurs a parasite power in the form of an enhanced induced power. Having raised this point I cannot resolve it, however, and so will follow convention and ignore the parasite power requirement.

The total power expended in moving the wings against their aerodynamic forces was defined in paper V as the product of the flapping velocity U and the 'total' wing drag – that component of the net aerodynamic force which is parallel to U. There are two contributions to the total drag: the profile drag, which results from the skin friction and pressure drag of the wing profile, and the induced drag, which depends on the induced velocity of the wake vorticity shed in association with circulatory lift. The total aerodynamic power can be estimated directly from a blade-element analysis based on the *flapping* velocity if the *total* drag coefficient is measured experimentally; this involves the extremely difficult task of re-creating accurately the pattern of wake vorticity shed by the flapping wing. A more practicable alternative is to separate this power into its two components, using the vortex theory of paper V to calculate the *induced power* P_{ind}, and a blade-element analysis based on the *relative* velocity and the *profile* drag coefficient $C_{D,pro}$ to evaluate the *profile power* P_{pro}.

Flapping flight also requires power to accelerate and decelerate the wings, P_{acc}. When averaged over a half-stroke, this *inertial power* must be zero according to a mechanical definition because there is no net acceleration of the wings. The flight muscles cannot exploit this nicety, however, and must consume some metabolic energy when doing 'negative' work to decelerate the wings. The use of elastic structures to store the kinetic energy of the oscillating wings obviously reduces this power demand, and will be discussed in §4.2.5. and 4.2.6.

3.1. *Induced power*

The vortex theory of paper V estimates the induced power from the energy per unit time imparted to the vortex wake. The *mean specific induced power* $\overline{P^*_{ind}}$ $(= \overline{P_{ind}}/mg)$ is given by equation (V. 42) as

$$\overline{P^*_{ind}} = P^*_{RF}(1+\sigma+\tau), \tag{20}$$

where the mean is taken over the period $1/n\hat{f}$ of the lift impulse. $\overline{P^*_{ind}}$ can be calculated separately for the two half-strokes when both provide mass support ($\hat{f} = 2$), but the values are unlikely to differ significantly; equation (20) can thus be used for the mean value over the wingbeat period. From equation (V. 15), the Rankine–Froude estimate of the induced power is

$$P^*_{RF} = \left[\frac{2p_w}{\rho\Phi\mathcal{R}\cos\beta}\right]^{\frac{1}{2}}. \tag{21}$$

The temporal correction factor τ for the wake periodicity is defined by equation (V. 44),

$$\tau = 0.079\, s^2, \tag{22}$$

where the spacing parameter s can be calculated from equation (3). The spatial correction factor σ is a function of the circulation profile during the wingbeat, and it is given in equation (V. 43) as

$$\sigma = \frac{1}{\hat{I}^{\frac{3}{2}}} \int_{-1}^{1} \int_{0}^{1} \hat{\Gamma}^{\frac{3}{2}} \hat{r}\, \mathrm{d}\hat{r}\, \mathrm{d}\hat{\phi} - 1. \tag{23}$$

Substituting equations (7) and (9), we can derive σ for the quasi-steady lift mechanism;

$$\sigma(\overline{C_L}) = \frac{\sqrt{2}\overline{|\mathrm{d}\hat{\phi}/\mathrm{d}\hat{t}|^{\frac{5}{2}}} \int_{0}^{1} \hat{c}^{\frac{3}{2}} \hat{r}^{\frac{5}{2}}\, \mathrm{d}\hat{r}}{\hat{r}_2^3(S)\,[\overline{(\mathrm{d}\hat{\phi}/\mathrm{d}\hat{t})^2}]^{\frac{3}{2}}} - 1, \tag{24}$$

Substituting equations (15) and (16) instead, the spatial correction factor for rotational mechanisms is

$$\sigma(\overline{\gamma}) = \frac{\int_{0}^{1} \hat{c}^3 \hat{r}\, \mathrm{d}\hat{r}}{\sqrt{2}\hat{v}^{\frac{3}{2}} \hat{r}^3_1(v)} - 1. \tag{25}$$

The integrals in equations (24) and (25) can be interpreted as moment parameters of the wing shape similar to those defined in paper II.

3.2. *Profile power*

The poor state of our knowledge concerning the profile drag forces on flapping wings was emphasized in paper IV. Until the appropriate experimental studies are done we can only assume, as did Weis-Fogh (1972, 1973), that the profile drag obeys the usual quasi-steady relation (paper I). Thus the profile drag D'_{pro} on a flapping wing element will be taken as that corresponding to steady motion at the same instantaneous linear velocity and attitude:

$$D'_{\mathrm{pro}} = \tfrac{1}{2}\rho c U_{\mathrm{r}}^2 C_{\mathrm{D,pro}}. \tag{26}$$

The choice of a suitable profile drag coefficient $C_{\mathrm{D,pro}}$ should be guided by the wing profile, the angle of incidence, and the Reynolds number Re. Bearing in mind the scarcity of experimental results for animal wings, though, the choice of $C_{\mathrm{D,pro}}$ will actually be little more than an educated guess.

For the large angles of incidence used in hovering, $C_{\mathrm{D,pro}}$ is likely to be about 0.15–0.2 for Re equal to 1500, and 0.5 for Re equal to 200 (paper IV). The profile drag coefficient tends to vary inversely with the square root of the Reynolds number for Re less than several thousand, and the following approximation can thus be derived for that range:

$$C_{\mathrm{D,pro}} \approx \frac{7}{\sqrt{Re}}. \tag{27}$$

The Reynolds number of a wing element is proportional to cU, so it will vary along the wing and throughout the cycle in hovering. According to a strict interpretation of the quasi-steady assumption, values of $C_{\mathrm{D,pro}}$ for the blade-element equation (26) should be determined as a function of the instantaneous Re of the wing element. It is probably sufficient, however, to use a mean value $\overline{C_{\mathrm{D,pro}}}$ calculated from equation (27) for some representative mean value $\overline{Re}$ of

the Reynolds number. The definition of $\overline{Re}$ is quite arbitrary, but it should be biased somewhat towards the upper end of the range of Re over the cycle, as this is where the greatest profile drag occurs. I have therefore chosen a simple expression for $\overline{Re}$, based on the mean wing chord $\bar{c}$ and the mean wing tip velocity $\overline{U_t}$;

$$\overline{Re} = \frac{\bar{c}\overline{U_t}}{\nu} = \frac{4\Phi R^2 n}{\nu \mathcal{A}R}, \tag{28}$$

where ν is the kinematic viscosity for air.

The profile drag is parallel to the relative velocity, so the profile power P'_{pro} expended by a wing element against this drag force must be $D'_{\mathrm{pro}}\, U_{\mathrm{r}}$. By integrating along the lengths of the wing pair and averaging over the half-stroke, we can derive the total *mean specific profile power* $\overline{P^*_{\mathrm{pro}}}$ $(= \overline{P_{\mathrm{pro}}}/mg)$ based on a mean profile drag coefficient;

$$\overline{P^*_{\mathrm{pro}}} = \frac{\rho n^3 \Phi^3 R^3 \hat{r}_3^3(S)\, \overline{|\mathrm{d}\hat{\phi}/\mathrm{d}\hat{t}|^3 \cos^3\beta}}{16 p_{\mathrm{w}} \cos^3\beta_{\mathrm{r}}} \overline{C_{\mathrm{D,pro}}}, \tag{29}$$

where $\hat{r}_3^3(S)$ is the non-dimensional third moment of wing area (paper II), and $\overline{|\mathrm{d}\hat{\phi}/\mathrm{d}\hat{t}|^3}$ is the mean cube of the absolute value of the non-dimensional angular velocity (paper III). I have compared the results from equation (29) with the mean specific profile power based on instantaneous values of $C_{\mathrm{D,pro}}$, as mentioned above, and they differ by less than 7 %. This error is very acceptable, and probably less than that incurred by the quasi-steady assumption itself, so the use of a mean profile drag coefficient is quite justified.

In addition to the power requirement that it incurs, the profile drag may also be important in the *net force balance* of hovering, particularly for animals that use an inclined stroke plane. The quasi-steady blade-element equation (26) can be integrated along the wings and averaged over a half-stroke to find the *mean value of the magnitude* of the profile drag force, $\overline{D_{\mathrm{pro}}}$. Dividing this by mg, we obtain a non-dimensional equation of the same form as $\bar{L}$ for the quasi-steady lift mechanism:

$$\overline{\hat{D}_{\mathrm{pro}}} = \frac{\rho n^2 \Phi^2 R^2 \hat{r}_2^2(S)\, \overline{(\mathrm{d}\hat{\phi}/\mathrm{d}\hat{t})^2 \cos^2\beta}}{8 p_{\mathrm{w}} \cos^2\beta_{\mathrm{r}}} \overline{C_{\mathrm{D,pro}}}, \tag{30}$$

and

$$\frac{\bar{L}}{\overline{\hat{D}_{\mathrm{pro}}}} = \frac{\overline{C_{\mathrm{L}}}}{\overline{C_{\mathrm{D,pro}}}}. \tag{31}$$

The profile drag force on a wing element is a vector, though, and the lateral component of this force will be cancelled by that of the corresponding element on the opposite wing. The mean profile drag force $\overline{D}$ over the half-stroke will therefore be parallel to the plane of bilateral symmetry, and the *magnitude of the mean value* is given in non-dimensional form by

$$\bar{D} = \frac{\rho n^2 \Phi^2 R^2 \hat{r}_2^2(S)\, \overline{[(\mathrm{d}\hat{\phi}/\mathrm{d}\hat{t})^2 \cos\phi]\cos^2\beta}}{8 p_{\mathrm{w}} \cos^2\beta_{\mathrm{r}}} \overline{C_{\mathrm{D,pro}}}. \tag{32}$$

It proves useful to define a parameter δ such that

$$\bar{D} = \delta \overline{\hat{D}_{\mathrm{pro}}}, \tag{33}$$

where δ is the magnitude of the mean profile drag divided by the mean of the magnitude of the profile drag:

$$\delta = \overline{[(\mathrm{d}\hat{\phi}/\mathrm{d}\hat{t})^2 \cos\phi]} / \overline{(\mathrm{d}\hat{\phi}/\mathrm{d}\hat{t})^2}. \tag{34}$$

The value of δ is unlikely to be critically dependent on the details of the wing motion $\phi(t)$,

which is not very different from simple harmonic motion for the insects of paper III. Instead of calculating δ from the experimental results, it can therefore be estimated with small error by using simple harmonic motion in equation (34):

$$\delta \approx \frac{\int_0^{\frac{1}{2}} \sin^2(2\pi\hat{t}) \cos\left[\overline{\phi} + \tfrac{1}{2}\Phi \cos(2\pi\hat{t})\right] \mathrm{d}\hat{t}}{\int_0^{\frac{1}{2}} \sin^2(2\pi\hat{t})\, \mathrm{d}\hat{t}}. \tag{35}$$

δ is now a function of only the stroke angle Φ and the mean positional angle $\overline{\phi}$, and the results from equation (35) are presented in figure 1. It is clear that δ is not a very sensitive parameter, and ranges between 0.72 and 0.91 for the insects in paper III, so the estimate from equation (35) should be sufficiently accurate.

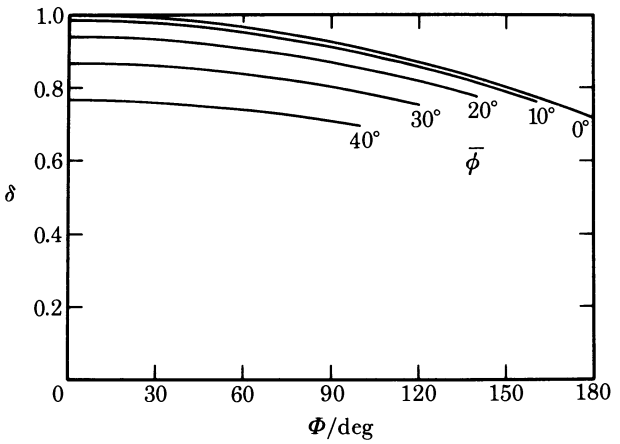

FIGURE 1. The parameter δ, which is the magnitude of the mean profile drag over a half-stroke divided by the mean magnitude of the profile drag, plotted against the stroke angle Φ for four values of the mean positional angle $\overline{\phi}$. Results for negative values of $\overline{\phi}$ are the same as for positive.

3.3. *Inertial power*

The inertial power required to accelerate the mass of a wing pair is given by the angular velocity $\mathrm{d}\phi/\mathrm{d}t$ multiplied by the inertial torque $I_{\mathrm{w}}(\mathrm{d}^2\phi/\mathrm{d}t^2)$, where I_{w} is the moment of inertia of the wing pair with respect to the wing bases. In Weis-Fogh's (1972, 1973) analyses of hovering flight, he assumed that the wings oscillated in simple harmonic motion and thus derived analytical expressions for the derivatives of ϕ with respect to t. Substantial errors can be expected in calculating $\mathrm{d}^2\phi/\mathrm{d}t^2$ from $\phi(t)$ measured experimentally, though, because of the manner in which experimental errors compound when taking derivatives. It would therefore be wise to limit our interests to the *mean* values of torque or power instead of attaching much significance to any instantaneous values, as Weis-Fogh did with the maximum torque. The temptation to discuss instantaneous values can be avoided by calculating the mean inertial power from the work done in accelerating the wing pair up to its maximum angular velocity during the first half of a half-stroke. This work is equal to the kinetic energy gained by the wing pair, $\frac{1}{2}I_{\mathrm{w}}(\mathrm{d}\phi/\mathrm{d}t)^2_{\mathrm{max}}$, and dividing by the period $1/4n$ of acceleration, we obtain the mean

inertial power $2nI_w(d\phi/dt)^2_{max}$. The moment of inertia I_w of the wing pair is equal to the second moment of wing mass, m_2, which is given by equations (II. 9) and (II. 11) as

$$m_2 = m_w R^2 \hat{r}_2^2(m) = \rho_w S R^3 \hat{h} \hat{r}_2^2(m), \tag{36}$$

where m_w is the mass of the wing pair, $\hat{r}_2^2(m)$ is the non-dimensional second moment, ρ_w is the wing density, and $\hat{h}$ is the mean wing thickness divided by the wing length.

The wing chord is nearly perpendicular to the stroke plane during the rapid accelerations and decelerations at either end of the wingbeat. The inertia of the wing will therefore be increased by the mass of air which it accelerates, leading to an apparent increase in the wing mass known as the virtual mass (paper II). For a wing element of spanwise width dr accelerated normal to its chord, the virtual mass is equal to the mass of air in an imaginary circular cylinder around the wing with the chord as the diameter: $\frac{1}{4}\rho\pi c^2 dr$. The virtual mass v of the wing pair is proportional to the mass of air in a cylinder of span $2R$ and diameter equal to the mean chord $\bar{c}$, and it is defined in equation (II. 13) as

$$v = 2\rho\pi R^3 \hat{v}/\mathcal{R}^2, \tag{37}$$

where the proportionality constant $\hat{v}$ depends on the wing shape. The moment of inertia v_2 for the virtual mass and its appropriate non-dimensional form $\hat{r}_2^2(v)$ is given by equation (II. 16):

$$v_2 = vR^2 \hat{r}_2^2(v) = \tfrac{1}{8}\rho\pi S^2 R \hat{v} \hat{r}_2^2(v). \tag{38}$$

The power required to accelerate the virtual mass has not been evaluated previously for flapping flight, but it will obey the same relation as the inertial power for the wing mass with m_2 replaced by v_2. The total *mean specific inertial power* $\overline{P^*_{acc}}$ required to *accelerate* the wing and virtual masses during the *first half* of a half-stroke is therefore

$$\begin{aligned}\overline{P^*_{acc}} &= 2n(m_2+v_2)(d\phi/dt)^2_{max}/mg \\ &= \frac{\rho n^3 \Phi^2 R^3 (d\hat{\phi}/d\hat{t})^2_{max}}{2p_w}\left[\frac{\rho_w}{\rho}\hat{h}\hat{r}_2^2(m) + \frac{\pi\hat{v}\hat{r}_2^2(v)}{2\mathcal{R}}\right].\end{aligned} \tag{39}$$

The power demands during deceleration in the second half of the half-stroke will be discussed in §4.2.4.

4. Results and discussion

Values for the morphological and kinematic parameters that appear in the equations of the preceding section are scattered throughout papers II and III, and have been collected here for quick reference. The nature of these parameters is such that they can be divided into two distinct groups – *gross parameters*, which are presented in table 1, and *shape parameters*, which are given in table 2. The gross morphological parameters offer what may be considered as a first order description of the animal: the wing loading, the wing length, the aspect ratio, the mean wing thickness (proportional to the wing mass), and the virtual mass of the wings. The gross kinematic parameters similarly provide a rough characterization of the wing motion using the stroke plane angle, the stroke angle, the wingbeat frequency, and the mean angular velocity of pronation and supination. In contrast, the shape parameters are determined by the normalized distributions of gross parameters, and furnish a second order description of the hovering process. These include the non-dimensional moments of wing area, virtual mass and wing mass, plus the first moment of $\hat{c}^3$ and the $\frac{5}{2}$ moment of $\hat{c}^{\frac{3}{2}}$, for which I can offer no physical

PHILOSOPHICAL TRANSACTIONS OF THE ROYAL SOCIETY B BIOLOGICAL SCIENCES

Table 1. Values of gross morphological and kinematic parameters for hovering insects

(Data taken from papers II and III, and the identification code ID is from paper II.)

insect	ID	$\frac{p_w}{N\ m^{-2}}$	$\frac{R}{mm}$	$\mathcal{R}$	$\hat{h}$ (%)	$\hat{v}$	$\frac{\beta}{rad\ [deg]}$	$\frac{\Phi}{rad\ [deg]}$	$\frac{n}{Hz}$	$\frac{\hat{\omega}}{rad}$
horizontal stroke plane										
Coccinella 7-punctata	LB04	4.76	11.2	7.07	0.104	1.08	0.31 [18]	3.09 [177]	53.9	14.8
Tipula obsoleta	CF02	1.89	12.7	10.9	0.0544	1.17	0.19 [11]	2.13 [122]	45.5	20.6
Tipula paludosa	CF04	4.54	17.4	11.3	0.0525	1.17	0.10 [6]	2.09 [120]	58.0	17.5
Episyrphus balteatus	HF07	6.54	9.3	8.45	0.0759	1.11	−0.03 [−2]	1.66 [95]	159	13.4
Eristalis tenax (figure 12, paper III)	DF01	9.23	11.4	7.15	0.106	1.09	0 [0]	1.90 [109]	157	9.6
Eristalis tenax (figure 13, paper III)	DF01	9.23	11.4	7.15	0.106	1.09	0.14 [8]	1.85 [106]	164	11.6
Apis mellifera	HB01	17.5	9.8	6.74	0.0760	1.07	−0.19 [−11]	2.27 [130]	197	9.6
Bombus hortorum	BB04	18.8	14.1	6.73	0.0543	1.10	−0.14 [−8]	2.09 [120]	152	9.6
Bombus lucorum	BB08	19.5	14.1	6.83	0.0692	1.10	0.10 [6]	2.27 [130]	140	9.6
inclined stroke plane										
Episyrphus balteatus (figure 10, paper III)	HF08	5.46	10.0	7.92	0.0691	1.12	0.37 [21]	1.15 [66]	141	13.1
Episyrphus balteatus (figure 11, paper III)	HF08	5.46	10.0	7.92	0.0691	1.12	0.56 [32]	1.20 [69]	144	13.1

PHILOSOPHICAL TRANSACTIONS OF THE ROYAL SOCIETY B BIOLOGICAL SCIENCES

TABLE 2. VALUES OF THE SHAPE PARAMETERS FOR THE INSECTS IN TABLE 1

(Data taken from papers II and III. Parameters involving $d\hat{\phi}/d\hat{t}$ are determined over the entire wingbeat cycle.)

ID	$\hat{r}_2^2(S)$	$\hat{r}_3^3(S)$	$\int_0^1 \hat{c}^{\frac{3}{2}}\hat{r}^{\frac{5}{2}}\,d\hat{r}$	$\hat{r}_1(v)$	$\hat{r}_2^2(v)$	$\int_0^1 \hat{c}^3\hat{r}\,d\hat{r}$	$\hat{r}_2^2(m)$	$\left\lvert\frac{d\hat{\phi}}{d\hat{t}}\right\rvert_{max}$	$\overline{\left\lvert\frac{d\hat{\phi}}{d\hat{t}}\right\rvert^2}$	$\overline{\left\lvert\frac{d\hat{\phi}}{d\hat{t}}\right\rvert^{\frac{5}{2}}}$	$\overline{\left\lvert\frac{d\hat{\phi}}{d\hat{t}}\right\rvert^3}$
horizontal stroke plane											
LB04	0.279	0.189	0.220	0.452	0.257	0.542	0.160	5.88	18.6	41.0	92.1
CF02	0.362	0.259	0.328	0.574	0.370	0.841	0.250	5.90	18.1	40.1	88.4
CF04	0.365	0.262	0.332	0.580	0.377	0.857	0.250	5.84	18.6	40.9	92.2
HF07	0.320	0.223	0.270	0.517	0.313	0.670	0.194	6.11	19.1	42.1	96.9
DF01 (figure 12, paper III)	0.285	0.195	0.225	0.457	0.259	0.549	0.160	6.45	19.1	43.5	100.5
DF01 (figure 13, paper III)	0.285	0.195	0.225	0.457	0.259	0.549	0.160	6.43	19.1	43.0	99.3
HB01	0.296	0.205	0.239	0.476	0.280	0.561	0.203	6.00	18.5	41.2	91.4
BB04	0.292	0.199	0.234	0.475	0.271	0.603	0.194	6.33	19.0	42.5	98.1
BB08	0.294	0.202	0.236	0.475	0.273	0.593	0.194	6.46	18.9	43.2	96.3
inclined stroke plane											
HF08 (figure 10, paper III)	0.319	0.221	0.269	0.519	0.312	0.690	0.194	6.37	19.2	43.2	99.1
HF08 (figure 11, paper III)	0.319	0.221	0.269	0.519	0.312	0.690	0.194	6.38	19.3	45.4	102.2

interpretation. The shape parameters for the wing motion are all functions of the absolute value of the non-dimensional angular velocity $\mathrm{d}\hat{\phi}/\mathrm{d}\hat{t}$: the maximum value, the mean square and mean cube, and the mean of $(\mathrm{d}\hat{\phi}/\mathrm{d}\hat{t})^{\frac{1}{2}}$.

Values of other parameters required for the numerical estimates of lift and power are as follows: the density ρ is 1.23 kg m^{-3} and the kinematic viscosity ν equals 1.46×10^{-5} m^2 s^{-1} for air at 15 °C and standard atmospheric pressure, and the density of wing cuticle ρ_w is about 1200 kg m^{-3} (paper II).

4.1. *Lift*

The average inertial forces from the wing mass and virtual mass must be zero over a half-stroke, so they make no contribution to the net force balance in hovering. The mean aerodynamic force, comprised of the mean circulatory lift $\overline{L}$ and the mean profile drag $\overline{D}$, must therefore be vertical and equal to mg when averaged over a wingbeat cycle. By using the subscripts d and u to denote the downstroke and upstroke respectively, and by defining the positive directions of the mean forces as illustrated in figure 2, the following two equations can be derived from the net force balance: the requirement of a net zero horizontal force gives

$$\overline{\hat{L}}_{\mathrm{d}} \sin \beta_{\mathrm{r,d}} - \overline{\hat{D}}_{\mathrm{d}} \cos \beta_{\mathrm{r,d}} + \overline{\hat{L}}_{\mathrm{u}} \sin \beta_{\mathrm{r,u}} + \overline{\hat{D}}_{\mathrm{u}} \cos \beta_{\mathrm{r,u}} = 0, \tag{40}$$

and for the vertical force to balance the animal's mass

$$\overline{\hat{L}}_{\mathrm{d}} \cos \beta_{\mathrm{r,d}} + \overline{\hat{D}}_{\mathrm{d}} \sin \beta_{\mathrm{r,d}} + \overline{\hat{L}}_{\mathrm{u}} \cos \beta_{\mathrm{r,u}} - \overline{\hat{D}}_{\mathrm{u}} \sin \beta_{\mathrm{r,u}} = 2, \tag{41}$$

where $\overline{\hat{D}}_{\mathrm{d}} = \delta\, \overline{\hat{D}_{\mathrm{pro,d}}}$ and $\overline{\hat{D}}_{\mathrm{u}} = \delta\, \overline{\hat{D}_{\mathrm{pro,u}}}$. These two equations can be used to determine $\overline{\hat{L}}_{\mathrm{d}}$ and $\overline{\hat{L}}_{\mathrm{u}}$, and hence the mean lift coefficient $\overline{C_{\mathrm{L}}}$ and the value of $\bar{\gamma}$ on the half-strokes. Different approximations can be employed depending on whether the stroke plane is horizontal or inclined, so the corresponding groups of insects will be treated separately.

4.1.1. *Lift coefficients*

(*a*) *Horizontal stroke plane.* Because of kinematic symmetry, we should expect nearly equal weight support on the half-strokes for animals hovering with a horizontal stroke plane. Values of β_{r} for this group have therefore been calculated with $\hat{f} = 2$, and they are presented in table 3. It is evident that β_{r} differs but little from the stroke plane angle β: typically β_{r} is 10° less than β on the downstroke and 10° greater on the upstroke. This small difference indicates that the relative velocity is primarily governed by the flapping velocity, and that the irregular helicoidal vortex sheet produced by circulatory lift is only slightly developed. Thus a planar representation of this vortex sheet in the relative stroke plane is quite justified (paper V).

The mean vertical force is derived almost entirely from lift for animals using a horizontal stroke plane, as can be seen in figure 2*a* for $\beta = 0$ and $\beta_{\mathrm{r}} = \pm 10°$. The lift force, which is perpendicular to the relative stroke plane, is tilted away from the vertical by only 10°; thus the difference between the magnitude of the mean lift and its vertical component, $\overline{L} \cos \beta_{\mathrm{r}}$, is less than 2%. A small component of the mean profile drag, $\overline{D} \sin \beta_{\mathrm{r}}$, subtracts from the mean vertical force, but this will be less than 4% for reasonable ratios of lift to profile drag, which will be, say, 4 at Re around 1000. For a perfectly horizontal stroke plane the mean lift over the cycle will therefore be underestimated by less than 6% if we simply equate it to mg and let β_{r} equal zero, reducing equation (41) to $\overline{\hat{L}}_{\mathrm{d}} + \overline{\hat{L}}_{\mathrm{u}} = 2$. This approximation will be used for all of the insects in table 3 even though the stroke plane angle β equals zero in only one case. β is typically small enough that the error of the approximation is not substantially increased, so

it will be assumed that β and β_r are zero for the purposes of calculation. In any case, β was affected by the almost continuous manoeuvres inside the flight chamber, and the value during 'true' hovering may not have been reported in paper III. This is certainly true for the ladybird *Coccinella 7-punctata* (LB04), which is included in the horizontal stroke plane group even though

TABLE 3. β_r, $\overline{C_L}$ AND $\bar{\gamma}$ FOR INSECTS WITH A HORIZONTAL STROKE PLANE

(Values of β_r are given separately for the downstroke and upstroke, but $\overline{C_L}$ and $\bar{\gamma}$ refer to both half-strokes.)

ID	$\beta_{r,d}$ deg	$\beta_{r,u}$ deg	$\overline{C_L}$	$\bar{\gamma}$
LB04	8	27	1.71	0.84
CF02	2	19	1.24	0.43
CF04	−2	14	0.97	0.41
HF07	−13	9	1.17	0.41
DF01 (figure 12, paper III)	−9	9	0.95	0.46
DF01 (figure 13, paper III)	−1	17	0.92	0.36
HB01	−20	−1	1.08	0.58
BB04	−17	2	1.10	0.53
BB08	−4	15	1.13	0.61

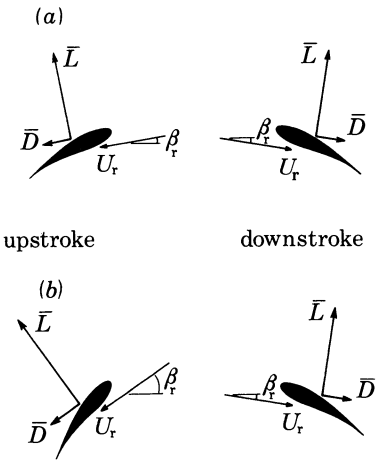

FIGURE 2. Directions of the aerodynamic force components on the downstroke and upstroke for (*a*) a horizontal stroke plane and (*b*) an inclined one.

β is 18°. In that film sequence the ladybird was steadily accelerating forwards and upwards, and the large value of β accounted for the forward acceleration. As explained in paper III, this sequence can be used to illustrate hovering by considering a more horizontal stroke plane and reducing β to a value characteristic of that group.

The mean lift coefficient on the downstroke must equal that on the upstroke if the value of $\overline{C_L}$ is to indicate the minimum lift coefficient compatible with hovering. $\overline{C_L}$ can then be calculated from equation (12) with $\bar{L} = 1$ and with the mean of $(\mathrm{d}\hat{\phi}/\mathrm{d}\hat{t})^2$ taken over *both* half-strokes; this mean value is also used in equation (19) for $\bar{\gamma}$. $\overline{C_L}$ and $\bar{\gamma}$ for the insects hovering with a horizontal stroke plane are presented in table 3, and will be discussed in §4.1.2. (*b*).

(*b*) *Inclined stroke plane.* Two of the film sequences from paper III show very precise hovering with an inclined stroke plane by the hover-fly *Episyrphus balteatus* (HF08). The stroke plane

angles are 21° and 32°, but there is no question of demoting the sequence with 21° to the horizontal stroke plane group; it provides an excellent view of 'true' hovering with no detectable accelerations. With the notable exception of U. M. Norberg (1976), studies on animals hovering with an inclined stroke plane have previously been hampered by incomplete data (Weis-Fogh 1973; R. Å. Norberg 1975; U. M. Norberg 1975), so the two hover-fly sequences will receive considerable attention.

If the half-strokes generate nearly equal weight support for the hover-fly, β_r can be estimated as before with $\hat{f} = 2$: the values of $\beta_{r,d}$ and $\beta_{r,u}$ are then 0° and 37° respectively for $\beta = 21°$, and 13° and 46° for $\beta = 32°$. The differences between β_r and β are more pronounced than for a horizontal stroke plane, about 20° on the downstroke and 15° on the upstroke. This is owing to a higher ratio of the induced velocity to the flapping velocity. The resulting directions of the mean force components are quite asymmetrical for the half-strokes, as shown in figure 2*b*. Downstroke lift is nearly vertical and thus suitably directed for weight support, but any lift on the upstroke produces a large horizontal thrust that would have to be balanced by an enhanced downstroke profile drag.

An extreme alternative is to minimize the upstroke lift and rely solely on the downstroke for weight support. If that is the case, then β_r for the downstroke should be calculated from equation (4) with s based on $\hat{f} = 1$. A different procedure is required for the upstroke, however, because equation (4) is only valid for half-strokes that provide weight support. Equation (4) is derived from equation (2), which assumes a mean induced velocity of $P^*_{RF}(1+\tau)$ during the half-stroke, where τ reflects the increase over the steady Rankine–Froude downwash caused by the impulsive vertical forces. This increase is presumably absent for a half-stroke not involved in weight support, so equation (2) should be used with $\tau = 0$ to estimate β_r for the upstroke. Values of $\beta_{r,d}$ and $\beta_{r,u}$ are then $-7°$ and 36° respectively for $\beta = 21°$, and 5° and 44° for $\beta = 32°$.

When we consider these two extreme cases, we see that the orientation of the relative stroke plane is not greatly influenced by the amount of weight support on the upstroke. The mean lift and profile drag on the downstroke are approximately vertical and horizontal, as for the horizontal stroke plane group. The directions of the mean force components on the upstroke, though, are always ill-suited for weight support; the mean profile drag contributes a substantial negative vertical force, and the mean lift has a large horizontal thrust component. However, a vertical force on the upstroke may be crucial for the hover-flies if the downstroke cannot generate sufficient lift.

The upstroke can, in fact, provide any amount of lift up to the limits of $C_{L,max}$ and γ_{max} as long as downstroke drag can cancel the resulting thrust. Thus it is clear that the net force balance for an inclined stroke plane may not be satisfied by unique values of the force coefficients, but the range of values can be investigated in the following manner. Using equations (40) and (41) of the force balance, plus equations (11), (30) and (33), we can derive

$$\overline{C_{L,u}} = \frac{1}{(1+\tan\beta_{r,u}\tan\beta_{r,d})}\left[\frac{16\,p_w\cos\beta_{r,u}}{\rho n^2\Phi^2R^2\hat{r}_2^2\,(S)\,\overline{(d\hat{\phi}/d\hat{t})^2}\cos^2\beta} + \delta\,(\tan\beta_{r,u}-\tan\beta_{r,d})\,\overline{C_{D,pro,u}} - \frac{\cos\beta_{r,u}}{\cos^3\beta_{r,d}}\overline{C_{L,d}}\right], \quad (42)$$

and

$$\overline{C_{D,pro,d}} = \frac{\tan\beta_{r,u}\cos\beta_{r,d}}{\delta\cos\beta_{r,u}}\overline{C_{L,u}} + \frac{\cos\beta_{r,d}}{\cos\beta_{r,u}}\overline{C_{D,pro,u}} + \frac{\tan\beta_{r,d}}{\delta}\overline{C_{L,d}}. \quad (43)$$

PHILOSOPHICAL TRANSACTIONS OF THE ROYAL SOCIETY B BIOLOGICAL SCIENCES

The surprising result is that the mean force coefficients on the upstroke and the downstroke are all related by simple linear functions. The mean rotational lift coefficient on the downstroke $\overline{\gamma}_{\mathrm{d}}$ can also be found as a linear function of $\overline{C_{\mathrm{L,d}}}$ from equation (19), and the value on the upstroke is simply given by the ratio

$$\frac{\overline{\gamma}_{\mathrm{u}}}{\overline{\gamma}_{\mathrm{d}}} = \frac{\overline{C_{\mathrm{L,u}}}\cos\beta_{\mathrm{r,u}}}{\overline{C_{\mathrm{L,d}}}\cos\beta_{\mathrm{r,d}}}. \tag{44}$$

The range of coefficients for the two hover-fly sequences will now be calculated. The values of δ obtained from equation (35) are 0.94 for $\beta = 21°$ and 0.89 for $\beta = 32°$. Judging from the previous estimates, $\beta_{\mathrm{r,d}}$ and $\beta_{\mathrm{r,u}}$ are likely to vary little with the amount of weight support provided by the upstroke; it will be shown that the upstroke probably supplies only a small force, though, so the estimates based on zero upstroke support will be used. The difference between the means of $(\mathrm{d}\hat{\phi}/\mathrm{d}\hat{t})^2$ on the half-strokes is within experimental error for the two sequences, and thus the mean value over the cycle can be used in equation (42). For the sequence with $\beta = 21°$, the equations then reduce to

$$\overline{C_{\mathrm{L,u}}} = 4.48 + 0.88\,\overline{C_{\mathrm{D,pro,u}}} - 0.91\,\overline{C_{\mathrm{L,d}}}, \tag{45}$$

$$\overline{C_{\mathrm{D,pro,d}}} = 4.24 + 2.06\,\overline{C_{\mathrm{D,pro,u}}} - 0.99\,\overline{C_{\mathrm{L,d}}}, \tag{46}$$

$$\overline{\gamma}_{\mathrm{d}} = 0.22\,\overline{C_{\mathrm{L,d}}}, \tag{47}$$

and

$$\overline{\gamma}_{\mathrm{u}} = 0.80 + 0.16\,\overline{C_{\mathrm{D,pro,u}}} - 0.17\,\overline{C_{\mathrm{L,d}}}. \tag{48}$$

For the sequence with $\beta = 32°$,

$$\overline{C_{\mathrm{L,u}}} = 3.53 + 0.72\,\overline{C_{\mathrm{D,pro,u}}} - 0.67\,\overline{C_{\mathrm{L,d}}}, \tag{49}$$

$$\overline{C_{\mathrm{D,pro,d}}} = 5.33 + 2.47\,\overline{C_{\mathrm{D,pro,u}}} - 0.91\,\overline{C_{\mathrm{L,d}}}, \tag{50}$$

$$\overline{\gamma}_{\mathrm{d}} = 0.21\,\overline{C_{\mathrm{L,d}}}, \tag{51}$$

and

$$\overline{\gamma}_{\mathrm{u}} = 0.54 + 0.11\,\overline{C_{\mathrm{D,pro,u}}} - 0.11\,\overline{C_{\mathrm{L,d}}}. \tag{52}$$

The mean force coefficients have been expressed in terms of the mean profile drag coefficient on the upstroke because it can be assigned a fairly reliable range of values from the quasi-steady profile drag assumption. $\overline{C_{\mathrm{D,pro,u}}}$ cannot be less than the minimum drag coefficient of the profile, $C_{\mathrm{D,min}}$, which is about 0.20 for the two sequences based on equation (IV. 9) with $\overline{Re}$ from equation (28). The maximum quasi-steady drag coefficient $C_{\mathrm{D,max}}$ of the wings must be similar to that of a flat plate with the chord perpendicular to its motion, around 1.2 for aspect ratios less than 10 at Re near 10^3 (Fage & Johansen 1927; Hoerner 1958). $\overline{C_{\mathrm{L,u}}}$ and $\overline{C_{\mathrm{D,pro,d}}}$ are thus plotted against $\overline{C_{\mathrm{L,d}}}$ for $\beta = 21°$ and $\beta = 32°$ in figure 3 and figure 4, respectively, using $C_{\mathrm{D,min}}$ and $C_{\mathrm{D,max}}$ to define the limits of $\overline{C_{\mathrm{D,pro,u}}}$.

The minimum mean coefficient required for hovering occurs when $\overline{C_{\mathrm{L,d}}} = \overline{C_{\mathrm{L,u}}}$, as for the horizontal stroke plane group. Depending on the assumed value of $\overline{C_{\mathrm{D,pro,u}}}$, this lift coefficient ranges between 2.44 and 2.90 for $\beta = 21°$, and 2.20 and 2.63 for $\beta = 32°$. However, the mean profile drag coefficient on the downstroke needed to balance the large horizontal thrust from the upstroke lift is between 2.23 and 3.84 for $\beta = 21°$, and 3.82 and 5.90 for $\beta = 32°$. These values are far too large for the quasi-steady profile drag assumption and, unless this assumption is rejected, we must conclude that the mean lift coefficient cannot be the same on the downstroke and upstroke.

PHILOSOPHICAL TRANSACTIONS OF THE ROYAL SOCIETY B BIOLOGICAL SCIENCES

To reduce the value of $\overline{C_{D,pro,d}}$ to a reasonable range the upstroke lift and hence $\overline{C_{L,u}}$ must be decreased, and $\overline{C_{L,d}}$ will then increase correspondingly. On imposing the restrictions of $C_{D,min}$ and $C_{D,max}$ on $\overline{C_{D,pro,d}}$ we obtain the small shaded area in the bottom right-hand corner of each figure, which represents the limits from the quasi-steady drag assumption. The minimum value of $\overline{C_{L,d}}$ consistent with that assumption is thus determined by $\overline{C_{D,pro,d}} = C_{D,max}$ and $\overline{C_{D,pro,u}} = C_{D,min}$, giving a value of 3.48 for $\beta = 21°$ and 5.08 for $\beta = 32°$. The result for $\beta = 32°$ is particularly interesting because the corresponding value of $\overline{C_{L,u}}$ is quite

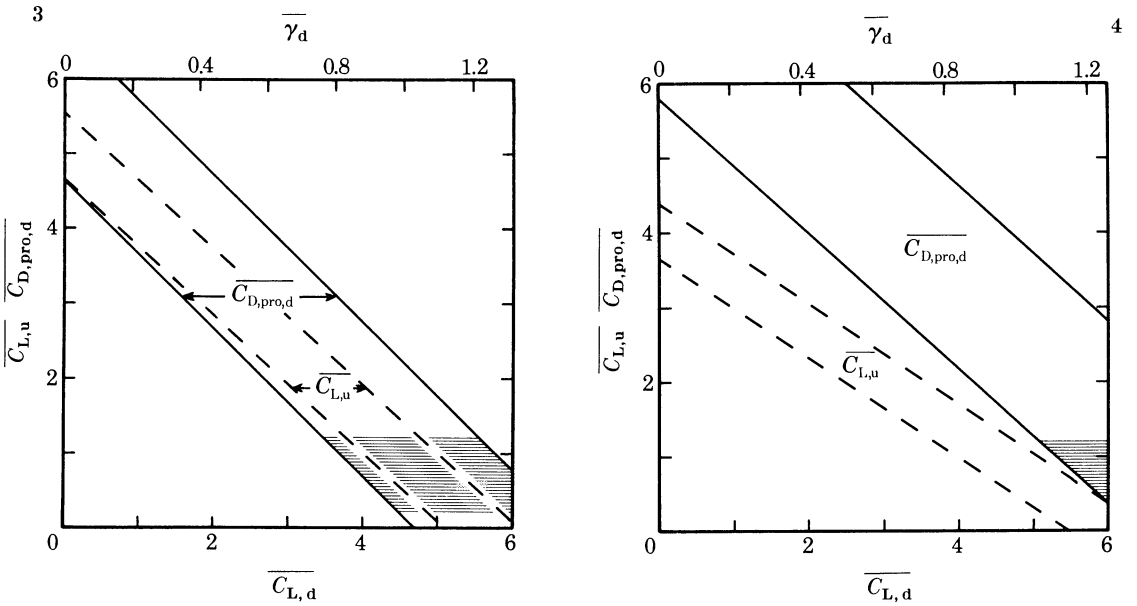

FIGURE 3. Mean force coefficients for the hover-fly (HF08) using an inclined stroke plane with $\beta = 21°$. $\overline{C_{L,u}}$ and $\overline{C_{D,pro,d}}$ are shown by dashed and solid lines, respectively, and are linear functions of both $\overline{C_{L,d}}$ and $\overline{C_{D,pro,u}}$. According to the quasi-steady profile drag assumption, $\overline{C_{D,pro,u}}$ must lie between $C_{D,min}$ and $C_{D,max}$; the left-hand line of each pair represents the limit imposed by $C_{D,min}$, and the right-hand line indicates $C_{D,max}$. The shaded area in the bottom corner is obtained by applying these limits to $\overline{C_{D,pro,d}}$ as well. The mean rotational lift coefficient on the downstroke $\overline{\gamma_d}$ depends on $\overline{C_{L,d}}$ alone, as shown on the upper axis of the figure.

FIGURE 4. Mean force coefficients for the hover-fly (HF08) using an inclined stroke plane $\beta = 32°$. Construction of the diagram is identical to figure 3.

small, about 0.27; the mean lift coefficient on the downstroke is therefore a minimum when the upstroke generates but little force. By reducing $\overline{C_{L,u}}$ below 0.27, $\overline{C_{D,pro,d}}$ can be decreased substantially from $C_{D,max}$ with only a small increase in $\overline{C_{L,d}}$, but I do not think this is practicable: the mean profile drag coefficient on the downstroke must be close to the maximum value if the wings are to produce a lift coefficient around 5.

For the sequence with $\beta = 21°$, the minimum value of $\overline{C_{L,d}}$ consistent with the drag assumption corresponds to $\overline{C_{L,u}}$ equal to 1.49. The mean profile drag coefficient on the upstroke must be greater than $C_{D,min}$ if that much lift is produced, however, and the value of 0.29 predicted by equation (27) is probably a better estimate for $\overline{C_{D,pro,u}}$. If it is accepted that $\overline{C_{D,pro,d}}$ is about 1.2 when $\overline{C_{L,d}}$ equals 5.08 for $\beta = 32°$, we can assume the same ratio of

lift to profile drag on the downstroke when $\beta = 21°$. Thus $\overline{C_{D,pro,d}}$ is approximately $\frac{1}{4}\,\overline{C_{L,d}}$ and, on substituting this into equation (46), we find that $\overline{C_{L,d}}$ is 3.93, $\overline{C_{L,u}}$ is 1.16, and $\overline{C_{D,pro,d}}$ is 0.94 when $\overline{C_{D,pro,u}}$ equals 0.29.

These solutions to the net force balance for the two hover-fly sequences seem the most plausible according to the quasi-steady profile drag assumption, and are summarized in table 4. The drag assumption has not been verified experimentally, though, and the results must be treated with caution. Even if it is verified in the future, it should be noted that the estimation of $\overline{C_{D,pro,d}}$ from the net force balance is quite prone to error because of the $\overline{C_{L,d}}$ tan $\beta_{r,d}$ term in equation (43). A small change in the relative stroke plane angle on the downstroke, which is only given approximately by equation (4), easily leads to substantial differences in the horizontal component of the downstroke lift and thus affects the mean profile drag coefficient.

TABLE 4. FORCE COEFFICIENTS FOR AN INCLINED STROKE PLANE

(These estimates for the two hover-fly (HF08) sequences showing an inclined stroke plane (figures 10 and 11, paper III) are based on assumed limits to the quasi-steady profile drag.)

β/deg	21	32
$\beta_{r,d}$/deg	−7	5
$\beta_{r,u}$/deg	36	44
$\overline{C_{L,d}}$	3.93	5.08
$\overline{C_{L,u}}$	1.16	0.27
$\overline{C_{D,pro,d}}$	0.94	1.2
$\overline{C_{D,pro,u}}$	0.29	0.20
$\overline{\gamma_d}$	0.86	1.07
$\overline{\gamma_u}$	0.21	0.04

4.1.2. *Aerodynamic mechanisms*

(*a*) *Inclined stroke plane.* In spite of these uncertainties concerning the profile drag, we can definitely conclude that the quasi-steady mechanism of *lift* production cannot meet the requirements of the hover-fly using an inclined stroke plane. $\overline{C_L}$ on the downstroke is likely to be about 3.9 for $\beta = 21°$ and 5.1 for $\beta = 32°$, and these values do not drop below 2.4 and 2.2 respectively even if C_L is taken as constant over the *cycle* by relaxing the upper limit to $\overline{C_{D,pro,d}}$. For the quasi-steady explanation of lift to be valid, the mean lift coefficient must not exceed the maximum value $C_{L,max}$ measured under steady-state conditions. Experimental values of $C_{L,max}$ were discussed in papers I and IV, and they range from 0.8 to 1.3 for insect wings. Thus the quasi-steady mechanism is insufficient even as an approximation to the aerodynamic forces for the hover-fly, as predicted by Weis-Fogh (1973), and unsteady effects must be involved.

The pied flycatcher *Ficedula hypoleuca* and the long-eared bat *Plecotus auritus* also hover using an inclined stroke plane with β near 30°, and their aerodynamics have been studied by U. M. Norberg (1975, 1976). She used the traditional Rankine–Froude theory with a disc area equal to πR^2 to calculate the induced velocity, which can seriously under-estimate the value compared with the new vortex theory of paper V. Some of my calculations for these animals (Ellington 1980) were based on her estimates, and will be modified here to bring them up to date. When the vortex theory is used, β_r on the downstroke is −12° for *Ficedula* and 9° for *Plecotus*. Thus the mean lift on the downstroke must be largely responsible for weight support,

PHILOSOPHICAL TRANSACTIONS OF THE ROYAL SOCIETY B BIOLOGICAL SCIENCES

as with the hover-fly, and a rough estimate of $\overline{C_{L,d}}$ can be obtained readily from equation (12) with $\bar{L} = 2$ and β_r as above. $\overline{C_{L,d}}$ is then 6.0 for *Ficedula* and 4.3 for *Plecotus*, which are similar to the values Norberg calculated, and far too large for the quasi-steady lift mechanism. It should be noted that the morphological and kinematic data for *Ficedula* were from different animals, and the rather high value of $\overline{C_{L,d}}$ may be because of this.

The conclusion that quasi-steady aerodynamics cannot explain the lift forces required by the hover-fly is also supported by kinematic observations. The geometrical angle of attack α of the wings is relatively constant for most of each half-stroke, and values at 0.7 R obtained by visual estimation were presented in paper III; for $\beta = 21°$, α is 35–40° over most of the downstroke and upstroke, and for $\beta = 32°$ it is 40–45° on the downstroke and 35–40° on the upstroke. The effective angle of attack α_r measured with respect to the relative velocity is $\alpha - (\beta - \beta_r)$ on the downstroke and $\alpha + (\beta - \beta_r)$ on the upstroke, and this gives values of about 10° and 22° respectively for $\beta = 21°$, and 15° and 25° for $\beta = 32°$. According to a quasi-steady explanation, these observations predict that the mean lift and profile drag on the upstroke are *greater* than on the downstroke – an impossible conclusion in light of the net force balance.

Which unsteady mechanism is the most likely candidate for providing the excessive lift required on the downstroke? The delayed stall of translation is the only conventional unsteady mechanism that can produce circulatory lift greater than the maximum value for steady motion, and it seemed a promising candidate in paper IV. However, the effective angles of attack observed for the hover-fly are probably too small for delayed stall to be useful. In any case, delayed stall would still produce greater forces on the upstroke and hence violate the net force balance.

It is very interesting to compare these two sequences of HF08 with that of another hover-fly (HF07), which hovered with a horizontal stroke plane. Together, they provide a series with β equal to −2°, 21°, and 32°, and so should reveal any kinematic differences between the types of hovering. The angle of attack is slightly reduced for the horizontal stroke plane, about 30–35° on both half-strokes, giving an effective angle of attack around 21° on the downstroke and upstroke. The mean lift coefficient required for HF07 is 1.17 (table 3); this is within the expected limits of $C_{L,max}$ if the Wagner effect is not too serious. Thus HF07 needs about $\frac{1}{3}$–$\frac{1}{4}$ of the lift required for the HF08 sequences, but the effective angles of incidence are not very different. It seems most improbable that any lift mechanism depending primarily on the effective angle of attack of the translating wings can explain these results.

If the aerodynamic differences between the hover-fly sequences cannot be accounted for in the translational phases of the cycle, we must turn our hopes to the rotational mechanisms, which may create circulation *before* translation and thus avoid the usual limits of $C_{L,max}$. The mean rotational lift coefficient $\bar{\gamma}$ for HF07 is 0.41 on both half-strokes; for HF08 with $\beta = 21°$ it is likely to be 0.86 on the downstroke and 0.21 on the upstroke, and for $\beta = 32°$ the respective values are 1.07 and 0.04 (table 4). However, we have no concrete values of γ_{max} to compare these with. The maximum value of γ should depend on the conditions of wing rotation, such as the separation distance between the opposing wings and the effective axis of rotation relative to the air. The fling and peel mechanisms probably generate the most circulation, with γ about 1.9 based on Maxworthy's (1979) experimental investigation of the fling and the inviscid analysis of the peel by Williamson & Ellington (paper IV). These two mechanisms could easily supply more lift than is needed by the hover-fly, but its wings rotate in *isolation* instead of close proximity.

The aerodynamic events during isolated rotation were discussed in paper IV, but there are

many uncertainties at present. The two major problems are (i) how much vorticity is created by the rotating wing, and (ii) how much of this vorticity remains 'bound' to the wing for the subsequent half-stroke, providing the circulation required for lift. Assuming that the wing rotates about the $\frac{1}{4}$ chord axis, equation (IV. 10) indicates that γ could be about 1.6. This circulation is of the wrong sense to generate the desired lift on the following half-stroke, but an equal amount of vorticity of the correct sense must be shed as a 'starting vortex' for the rotational motion. If that starting vorticity can be shed near the leading edge, the roles of bound and shed vorticity may be reversed on the subsequent half-stroke; the shed vorticity of rotation then becomes the bound circulation for lift. This mechanism is highly speculative, of course, but it does provide a means of using the strong vorticity that *must* be created during rotation. We should not expect γ for the subsequent half-stroke to be as high as 1.6, because the spatial partitioning of the rotational vorticity cannot be perfect, but if the wing can recover only $\frac{2}{3}$ of the 'correct' vorticity shed during rotation then it would satisfy the demands of the hover-fly downstroke with $\beta = 32°$.

To recover the shed vorticity it is essential that the leading edge rotates faster with respect to the air than the trailing edge, concentrating the shed vorticity near the leading edge. The hover-fly sequences are particularly interesting in view of this, because pronation is delayed and overlaps the beginning of the downstroke as the stroke plane becomes more inclined (figures 9, 10 and 11 in paper III); in fact, this is the most striking kinematic difference between the horizontal and inclined stroke planes apart from the gross changes in the stroke angle Φ. Given the same wing flexing, this delay causes the trailing edge to become stationary with respect to the air at an earlier stage of rotation because of the additional motion from translation. Thus the phase shift may partition the rotational vorticity between the half-strokes, as discussed in paper IV: more vorticity is shed at the leading edge as pronation is delayed, creating a larger downstroke circulation.

(*b*) *Horizontal stroke plane*. Although the quasi-steady lift mechanism does not work for HF08, it cannot be dismissed for HF07 using a horizontal stroke plane, where $\overline{C_L}$ is about 1.2. What about the other insects that hover with a horizontal stroke plane? With only two exceptions, $\overline{C_L}$ for these insects (table 3) range from 0.9 to 1.1, which is similar to the range calculated by Weis-Fogh (1973). These values are probably small enough to be accounted for by the quasi-steady assumption even allowing for the Wagner effect. However, the ladybird *Coccinella 7-punctata* (LB04) requires $\overline{C_L}$ equal to 1.7, which is greater than any value of $C_{L,\max}$ measured for insect wings, and the crane-fly *Tipula obsoleta* (CF02) needs 1.2, which is over 40 % above $C_{L,\max}$ determined for another tipulid *T. oleracea* (Nachtigall 1977). Even allowing for experimental errors, these values must contradict the quasi-steady assumption when the Wagner effect is taken into account, and thus two insects that hover with a horizontal stroke plane rely on unsteady effects.

The effective angle of attack α_r for the ladybird is about 25° on both half-strokes. The same value is found for the drone-fly *Eristalis* (DF01) in figure 13 of paper III, the honey bee *Apis mellifera* (HB01), and the bumble bees *Bombus hortorum* (BB04) and *B. lucorum* (BB08). It is therefore unlikely that the excessive lift coefficient for the ladybird is due to delayed stall at an increased angle of attack. For the crane-fly (CF02) α_r is 16° on the downstroke and 27° on the upstroke, compared with 27° and 37° respectively for the other crane-fly *T. paludosa* (CF04). Any mechanism based on the effective angle of attack would thus predict a higher $\overline{C_L}$ for CF04 instead of the lower one found.

As for the hover-fly using an inclined stroke plane, we are again forced to turn to the

rotational phases of the wingbeat to explain the extra lift of the ladybird and crane-fly (CF02). The wings of the ladybird are in close proximity while rotating: during pronation the trailing edges actually touch in the basal wing area and are separated by about $\frac{1}{4}$ of the mean chord $\bar{c}$ near the wing tip, but during supination they are slightly more separated and do not touch. Thus the ladybird performs a 'near fling' along most of the wing length, with a 'partial fling' in the basal area during pronation. It was argued in paper IV that these variations on the fling should also create circulation during rotation, but with a reduced effectiveness. The mean rotational lift coefficient for the ladybird is 0.84; this allows for a generous reduction of the 1.9 available from a complete fling or peel.

The crane-fly (CF02) wings are separated by about $\frac{1}{4}\bar{c}$ near the wing base in pronation, but the separation is greater than the mean chord for distal wing areas. Thus the events during pronation should be those of a near fling for basal wing areas, merging into isolated rotation with little wing interference for the distal half of the wing. The wings are completely separated in supination, though, so any net circulation created by pronation and supination should be primarily due to isolated rotation. A pronounced flexion is clearly evident along the chord as the wings rotate (figures 18 and 25*b* in paper III), which makes the trailing edge stationary with respect to the air in the latter half of rotation. As with delayed pronation for the hover-fly with an inclined stroke plane, this 'flex mechanism' (paper IV) might partition the vorticity shed during rotation such that some of it can be recovered for the following half-stroke. Indeed, the wing flexing also occurs for the hover-fly, and should increase the effectiveness of delayed pronation in partitioning the rotational vorticity. If the flex mechanism is feasible its mean rotational coefficient should be less than the other cases considered, but we have no idea what γ might be. CF02 requires $\overline{\gamma}$ equal to 0.43, only $\frac{1}{4}$ of the vorticity likely to be shed during isolated rotation, so we are not really asking for much.

Even a tentative rejection of the quasi-steady mechanism for CF02 leads to a striking conclusion for the remaining insects in table 3 that hover with a horizontal stroke plane. Their values of $\overline{C_L}$ are possibly within the limits of $C_{L,max}$, but I cannot find any differences between their kinematics and those of CF02 that would substantially influence the force coefficients. If the kinematics of the honey bee, bumble bees, drone-fly, hover-fly (HF07) and the other crane-fly (CF04) are basically the same as crane-fly CF02, we cannot accept the quasi-steady mechanism for them while rejecting it for CF02. This leads to the opposite conclusion from Weis-Fogh's, and does not support his claim that 'most insects perform normal hovering [i.e. with a horizontal stroke plane] on the basis of the well-established principles of steady-state flow', (Weis-Fogh 1973). It seems more likely that they use a rotational mechanism similar to that of CF02; indeed, values of $\overline{\gamma}$ for the remaining insects of table 3 are in a plausible range of 0.4–0.6. CF02 falls in the lower end of this range, in fact, and therefore is not exceptional if it uses a rotational lift mechanism instead of a quasi-steady one. Flexion of the wing during rotation is similar for CF02 and the other insects, so it would be appropriate to suggest that the flex mechanism operates for them as well.

Maxworthy (1981) has published a concise review of the fluid dynamics of insect flight, in which the importance of rotational effects also figure prominently in his discussion of hovering. Based on his earlier experimental studies (Maxworthy 1979; see paper IV), he concludes that unsteady effects must be substantial for isolated wing rotation. He found that the vorticity shed as a flat wing model slows down and rotates, interacts with the wing at the beginning of the following half-stroke, and forms a large leading edge bubble that provides

circulatory lift earlier than one would expect from the Wagner effect combined with the quasi-steady mechanism. Details of the vortex shedding could not be determined from that study, but it is clear that something akin to my isolated rotation must be happening. Savage *et al.* (1979) also found strong vortex shedding during rotation of a flat wing model although, as discussed in paper IV, this vorticity could not be 'recovered' for the following half-stroke because of the effective axis of rotation they used and the lack of coupling between the rotational and translation phases.

These two experimental studies certainly ease the path towards the conclusion that most, if not all, hovering animals rely primarily on rotational lift mechanisms instead of quasi-steady aerodynamics, as Weis-Fogh claimed. In fact, one animal can even be found in Weis-Fogh's (1972, 1973) studies that violates his conclusion: the hummingbird *Amazilia*, which was taken as a typical example of hormal hovering. He calculated a mean lift coefficient of 1.8 for *Amazilia*, and decided that this might be possible under quasi-steady conditions. I questioned that decision in paper I, however, based on the available measurements of $C_{L,max}$ for bird wings. By using the analysis of *Amazilia*'s wing shape from paper II, which is more accurate than Weis-Fogh's approximate method, I have recalculated $\overline{C_L}$ as 2.3 from equation (12) and his kinematic data. This value is much larger than the measurements of $C_{L,max}$ and clearly violates the quasi-steady assumption. As with the crane-fly CF02, if but one member of a homogeneous group disproves the assumption, then we must reject it for that entire group of animals using normal hovering.

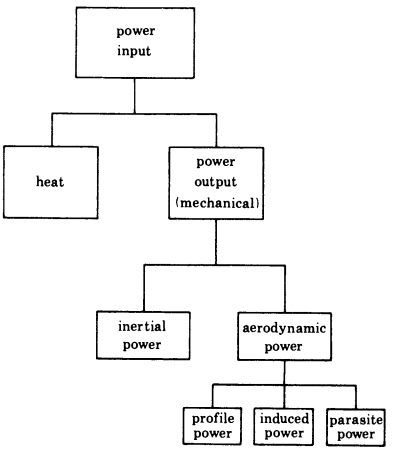

FIGURE 5. Pathway for the power expenditure in flapping flight. The mechanical power output of the flight muscles, composed of the inertial power and the components of the aerodynamic power, plus the heat produced must equal the metabolic power input. From Casey (1981*a*).

4.2. *Power*

Investigations of the lift mechanisms are vital to our understanding of how animals fly, but many biologists are more directly concerned with the energetic costs of flight. The power budget for a flying animal is best appreciated in diagrammatic form, as shown in figure 5. Some of the metabolic power input to the flight muscles appears as a mechanical power output, but most of it is degraded into heat by muscular inefficiency. The mechanical power output is divided into any inertial power required to accelerate and decelerate the wings, and the total aerodynamic power needed to move the wings and the body through the air. The aerodynamic

power in turn represents the sum of three distinct components: induced, profile and parasite powers. As already mentioned, the parasite power required to move the body through the air is commonly neglected for hovering flight.

Starting at the bottom of the figure, the individual power components will be investigated using the equations for power derived earlier. These components will then be combined with due regard to the influence of elastic storage on inertial power, and the resulting mechanical power output compared with measured metabolic rates to estimate the efficiency of the flight muscles. As before, it is assumed that β and β_r equal zero for the horizontal stroke plane group.

4.2.1. *Mean induced power*

The mean specific induced power $\overline{P^*_{ind}}$ is readily calculated from equations (20)–(25). When estimating the spacing parameter s, we again let $\hat{f}$ equal 2 and 1 for the horizontal and inclined stroke planes respectively. This will slightly overestimate the temporal correction factor τ for HF08 with $\beta = 21°$, because the upstroke does provide a little weight support, but integer values of $\hat{f}$ are required for the vortex theory. For the horizontal stroke plane group, the mean value of σ $(\overline{C_L})$ over the wingbeat *cycle* is obtained by using $(d\hat{\phi}/d\hat{t})^2$ and $|d\hat{\phi}/d\hat{t}|^{\frac{5}{2}}$ averaged over the cycle in equation (24). These functions should be averaged only over the supporting downstroke for HF08, but the means over the half-strokes are not significantly different from those over the cycle; mean values over the cycle can therefore be used for the downstroke in equation (24). The values of σ, τ and $\overline{P^*_{ind}}$ presented in table 5 are thus mean values over the cycle.

The striking result, predicted from momentum arguments in paper V, is that the spatial correction factor σ is quite insensitive to the aerodynamic mechanism generating lift. The value of σ for the rotational mechanisms, $\sigma(\overline{\gamma})$, is generally a small percentage higher than for the quasi-steady mechanism, $\sigma(\overline{C_L})$, but both require only about 10% more induced power than the simple Rankine–Froude estimate. The temporal correction factor τ is also small for the horizontal stroke plane group, indicating that the power losses caused by wake periodicity are about 5% of the power required for a perfectly steady Rankine–Froude jet. However, these losses are substantial for the hover-fly using an inclined stroke plane: about 50%. This is because the wake periodicity is markedly increased when weight support is provided by the downstroke alone.

Since the value of σ is small and insensitive, the calculated mean specific induced power over the cycle is virtually independent of the lift mechanism assumed: the difference between the two estimates of $\overline{P^*_{ind}}$ is typically less than 2%. Thus the uncertainties about the lift mechanism actually employed by hovering animals will not be reflected in the metabolic power requirements; this should please biologists more concerned with the energetics of flight rather than the aerodynamics. Indeed, the following rule-of-thumb predicts $\overline{P^*_{ind}}$ to within a small percentage for the insects using a horizontal stroke plane: $\overline{P^*_{ind}}$ equals 1.15 times the simple Rankine–Froude estimate P^*_{RF}.

The mean specific induced power over the cycle varies from 0.4 to 1.7 W N^{-1} for the insects in table 5. This range is slightly larger than would be predicted from the wing loading p_w, because the aspect ratio tends to decrease as p_w increases. Insects such as the crane-flies have a very low wing loading *and* disproportionately long wings; this reduces their disc loading (paper V) and hence their specific induced power. The largest values of $\overline{P^*_{ind}}$ occur for the honey bee and bumble bees, which have a high wing loading and low aspect ratio, and for the hover-fly paying a penalty in τ for its use of an inclined stroke plane.

PHILOSOPHICAL TRANSACTIONS OF THE ROYAL SOCIETY B BIOLOGICAL SCIENCES

TABLE 5. ESTIMATES FOR THE MECHANICAL POWER REQUIREMENTS OF HOVERING

ID	$\sigma(\overline{C_L})$	$\sigma(\overline{\gamma})$	τ	$\overline{P^*_{ind}(C_L)}$ W N^{-1}	$\overline{P^*_{ind}(\gamma)}$ W N^{-1}	$\overline{Re}$	$\overline{C_{D,pro}}$	$\overline{P^*_{pro}}$ W N^{-1}	$\overline{P^*_a}$ W N^{-1}	η_a	$\overline{P^*_{acc}}$ W N^{-1}
horizontal stroke plane											
LB04	0.07	0.13	0.08	0.69	0.72	810	0.25	0.45	1.15	0.52	2.09
CF02	0.11	0.08	0.05	0.42	0.41	390	0.35	0.61	1.03	0.35	1.92
CF04	0.09	0.09	0.04	0.63	0.63	896	0.23	0.90	1.53	0.37	3.94
HF07	0.07	0.09	0.05	0.98	1.00	736	0.26	0.96	1.95	0.45	6.44
DF01 (figure 12, paper III)	0.09	0.11	0.04	1.18	1.21	1,495	0.18	1.17	2.37	0.44	13.2
DF01 (figure 13, paper III)	0.08	0.11	0.04	1.19	1.22	1,519	0.18	1.20	2.41	0.44	14.1
HB01	0.09	0.09	0.05	1.56	1.56	1,757	0.17	1.16	2.72	0.50	10.4
BB04	0.08	0.13	0.06	1.67	1.74	2,568	0.14	0.99	2.70	0.55	9.72
BB08	0.10	0.12	0.06	1.65	1.68	2,543	0.14	0.96	2.63	0.54	10.5
inclined stroke plane											
HF08 (figure 10, paper III)	0.08	0.11	0.49	1.61	1.63	560	†	0.81	2.43	0.41	3.38
HF08 (figure 11, paper III)	0.13	0.11	0.52	1.73	1.70	598	†	0.88	2.60	0.37	3.94

† Values of the mean profile drag coefficient for HF08 are given in table 4.

Weis-Fogh (1972, 1973) did not explicitly estimate the induced power for his animals, but the results of table 5 can be compared with those of Rayner (1979). For animals using a horizontal stroke plane, Rayner suggests that $\overline{P^*_{\mathrm{ind}}}$ is approximately given by 1.04 P^*_{RF} in my terminology. The 'tip losses' due to wake periodicity are ignored in this approximation, so his correction to the Rankine–Froude estimate for the circulation profile during the wingbeat is about half my value ($\sigma \approx 0.1$). The 'impulse' correction he employed was criticized on conceptual grounds in paper V, however, and it should at first sight overestimate the total specific induced power by up to 30%. The reason it does not do so is because the initial rolled-up vortex ring area is also overestimated in his approximation, and these two errors cancel out. He neglected the changes in circulation with angular position of the wings and the reduced circulation near the wing base, both of which decrease the mean circulatory lift, and he concluded that the initial rolled-up ring area was about 92% of the area swept by the wings. If those factors are taken into account, my calculations from equations (9) and (16) show that this area is closer to 60%.

Rayner offers a similar correction that includes the effects of wake periodicity for animals using an inclined stroke plane. His term representing the spatial correction factor again yields a reasonable value (0.06) because of the same two overestimates mentioned above. However, his correction for wake periodicity is based on an initial ratio of the vortex core radius to the vortex ring radius of 0.17, and it was shown in paper V that such a large value violates momentum considerations in the limit of vanishing wake periodicity. This large core radius should underestimate the power required for a periodic wake, and his approximation gives $\overline{P^*_{\mathrm{ind}}}$ equal to 1.19 P^*_{RF} for HF08 with $\beta = 32°$, compared with my estimate of 1.63 P^*_{RF}.

4.2.2. *Mean profile power*

To calculate the mean specific profile power, we must first determine the mean Reynolds number from equation (28) and then select a suitable mean profile drag coefficient from equation (27). This coefficient is taken as constant during the wingbeat for insects with a horizontal stroke plane, so the mean of $|\mathrm{d}\hat{\phi}/\mathrm{d}\hat{t}|^3$ over the cycle is used in equation (29) to give $\overline{P^*_{\mathrm{pro}}}$ over the *cycle*. For the hover-fly HF08 the mean profile drag coefficients on the downstroke and upstroke have already been calculated in table 4. The mean of $|\mathrm{d}\hat{\phi}/\mathrm{d}\hat{t}|^3$ is not significantly different on the half-strokes for HF08, and the mean value over the cycle can be used in equation (29). $\overline{P^*_{\mathrm{pro}}}$ is then 1.03 W N^{-1} on the downstroke and 0.59 W N^{-1} on the upstroke for $\beta = 21°$, giving a mean value of 0.81 W N^{-1} over the cycle; for $\beta = 32°$ the values are 1.22, 0.54 and 0.88, respectively.

Table 5 includes the values of $\overline{Re}$, the mean profile drag coefficient, and $\overline{P^*_{\mathrm{pro}}}$ over the cycle. The mean specific profile power ranges from 0.5 to 1.2 W N^{-1}, and it is clearly of the same magnitude as $\overline{P^*_{\mathrm{ind}}}$ for a given insect. The results for HF08 are particularly interesting, because they reveal that the exceptionally large profile drag coefficients required on the downstroke of an inclined stroke plane do not incur a serious penalty in profile power. Indeed, $\overline{P^*_{\mathrm{pro}}}$ on the downstroke for HF08 is not much larger than for HF07 using a horizontal stroke plane, and $\overline{P^*_{\mathrm{pro}}}$ over the cycle is actually less. The relative velocity is considerably reduced on the downstroke of HF08 because of a smaller Φ and larger β, and this reduction offsets the big increase in $\overline{P^*_{\mathrm{pro}}}$ expected from the large profile drag coefficient.

4.2.3. *Aerodynamic efficiency*

The mean specific aerodynamic power $\overline{P^*_a}$ over the cycle is simply the sum of $\overline{P^*_{ind}}$ and $\overline{P^*_{pro}}$. By taking values from table 5, and by using the mean of $\overline{P^*_{ind}}$ calculated for quasi-steady and rotational mechanisms, the aerodynamic power ranges from 1.0 to 2.7 W N^{-1}. These estimates are similar to those of Weis-Fogh (1973), and three insects can be compared directly. For the crane-fly *Tipula*, the drone-fly *Eristalis*, and the honey bee *Apis* my values are 1.3, 2.5, and 2.8 W N^{-1} respectively, while his are 2.1, 2.3 and 2.1 W N^{-1}. This agreement is somewhat fortuitous, though, because he implicitly included the induced power twice in his estimate of $\overline{P^*_a}$. For the lift and drag coefficients in his blade-element analysis, 'we use polar diagrams from real wings so that the induced drag is taken into account automatically', (Weis-Fogh, 1972). This procedure is quite valid provided that the blade-element analysis is based on the *flapping* velocity, but he used the *relative* velocity instead. This was done explicitly in his paper of 1972, and implicitly in his 'corrected results' of 1973. The contribution of circulatory lift to the 'total' wing drag – the component of the net aerodynamic force that is parallel to the flapping velocity – is therefore counted twice, thus enhancing his values for the aerodynamic power. However, his total drag coefficients were strongly based on the results for locust forewings (Jensen 1956), which were shown to be improbably low in paper IV. His total drag coefficients are roughly equal to my profile drag coefficients predicted by equation (27), in fact, and this accounts for the agreement between our results.

The aerodynamic power represents the total energy per unit time imparted to the air by the wings. When it is considered that the goal of hovering is simply to provide a vertical force balancing the animal's weight, we can derive an *aerodynamic efficiency* η_a as the minimum power required to hover divided by the aerodynamic power actually expended (Weis-Fogh 1972). The minimum power occurs for a steady downward Rankine–Froude momentum jet, and is equal to P^*_{RF}; thus

$$\eta_a = \frac{P^*_{RF}}{\overline{P^*_a}} = \frac{P^*_{RF}}{\overline{P^*_{ind}} + \overline{P^*_{pro}}}. \tag{53}$$

Values of η_a are given in table 5 and range from 0.37 to 0.55. Weis-Fogh (1972) calculated similar aerodynamic efficiencies for a hummingbird and the fruit-fly *Drosophila*, and commented that these values were 'not bad' for an oscillating system. However, the effects of oscillation only appear in the temporal correction factor τ of $\overline{P^*_{ind}}$, and they are quite small in general. It would be more correct to conclude that these aerodynamic efficiencies are 'not bad' considering the enhanced profile power for wings operating at high angles of attack and low Reynolds numbers.

4.2.4. *Mean inertial power*

Having calculated the aerodynamic power, we need only estimate the inertial power requirement to arrive at the total mechanical power output of the flight muscles. The mean specific inertial power needed to *accelerate* the wing and virtual masses during the *first* half of a half-stroke is $\overline{P^*_{acc}}$, given by equation (39), and values are presented in table 5. The mean of $(\mathrm{d}\hat{\phi}/\mathrm{d}\hat{t})^2_{max}$ for the two half-strokes is used for this calculation, so $\overline{P^*_{acc}}$ can be regarded as the mean power required for the first half of either half-stroke. $\overline{P^*_{acc}}$ is substantially greater than $\overline{P^*_a}$, as also found by Sotavalta (1952) and Weis-Fogh (1972, 1973), revealing that the work

PHILOSOPHICAL TRANSACTIONS OF THE ROYAL SOCIETY B BIOLOGICAL SCIENCES

done in *accelerating* the wing and virtual masses is between 1.4 and 5.9 times the work done against aerodynamic forces over the same period. During the *second* half of the half-stroke, an equal but opposite mean power is obviously required to decelerate the wings, $-\overline{P^*_{\mathrm{acc}}}$. Although the mean aerodynamic power remains positive in that period, it is small compared with the magnitude of the power for deceleration and can be taken 'free' from the kinetic energy of the wings. Thus the *net* power requirement is negative over the second half of the half-stroke and equal to $-\overline{P^*_{\mathrm{acc}}}+\overline{P^*_{\mathrm{ind}}}+\overline{P^*_{\mathrm{pro}}}$. Active braking must therefore be done to absorb the excess kinetic energy of the wing and virtual masses.

How does this negative mechanical power fit into the net power budget? Indeed, this is a common problem for all types of oscillatory animal locomotion, except for swimming at very low Reynolds numbers. If the negative power is simply dissipated as heat and sound by some form of an end stop, then it can be ignored in the power budget, and the total mean specific mechanical power output required of the muscles is $\frac{1}{2}$ $(\overline{P^*_{\mathrm{acc}}}+\overline{P^*_{\mathrm{ind}}}+\overline{P^*_{\mathrm{pro}}})$ over the *cycle*. Alternatively, an elastic element could be stretched to brake the wings, storing the excess energy as elastic strain energy. This energy could then be released at the beginning of the following half-stroke, reducing the mechanical power demanded of the mucles. For perfect elastic storage the net inertial power requirement over the cycle is zero, and the mean mechanical power output of the muscle is just the aerodynamic power, $\overline{P^*_{\mathrm{ind}}}+\overline{P^*_{\mathrm{pro}}}$. In the absence of an elastic system or end stops, the wings must be decelerated by active tension in the flight muscles. This final solution demands that the muscles do 'negative' work; i.e. they are stretched while developing tension, instead of contracting as in 'positive' work. However, there seems little doubt that negative work uses considerably less metabolic energy than an equivalent amount of positive work for vertebrate striated muscle (Abbott *et al.* 1952; Asmussen 1952; Hill & Howarth 1959; Margaria 1968), and so the metabolic cost of negative work is often disregarded in animal locomotion studies. The muscles are therefore similar to an end stop, dissipating energy at a very small metabolic cost, and the total mean specific mechanical power output is again $\frac{1}{2}$ $(\overline{P^*_{\mathrm{acc}}}+\overline{P^*_{\mathrm{ind}}}+\overline{P^*_{\mathrm{pro}}})$ over the cycle.

4.2.5. *Elastic storage and mechanical power output*

Out of these three possibilities, Weis-Fogh (1972, 1973) calculated the mechanical power outputs during hovering based on the assumption that the muscles act as an end stop. He then compared these estimates with the available measurements of metabolic rate during flight, and concluded that an elastic system must be present in some insects because the mechanical efficiency of the flight muscles would be unreasonably high if the inertial power was included in their mechanical power output. He generalized and stated that 'the available evidence amounts to a circumstantial proof that as a group, flying insects possess and depend upon elastic forces in order to store and release the kinetic energy of the oscillating wings' (Weis-Fogh 1973). The importance of elasticity in insect flight was advocated over many years by Weis-Fogh (1959, 1961, 1965, 1972, 1973), and he identified three different materials for the construction of an elastic system: (i) the solid skeletal cuticle, (ii) elastomers such as the protein resilin, and (iii) an elastic component present in both neurogenic and myogenic flight muscles (Buchthal & Weis-Fogh 1956). It is now widely believed that the elasticity of active muscle residues in the cross-bridges (Huxley & Simmons 1971; Rack & Westbury 1974). For the neurogenic insects, Weis-Fogh noted that the major elastic stores were the cuticle of the thoracic box and the resilin-containing wing ligaments for locusts *Schistocerca gregaria* and a hawk moth *Sphinx ligustri*,

and the flight muscles themselves for a dragonfly *Aeschna grandis*. He did not suggest which structures might be most important for the myogenic insects, though. More recent calculations by Alexander & Bennet-Clark (1977) suggest that the elasticity of myogenic, or fibrillar, flight muscles should act as a major store for these insects. All of the insects in table 5 belong to orders that rely on fibrillar muscle, so this result is especially important here. I think that the case can be stated even more strongly, based on the contractile mechanics of fibrillar muscle, and suggest that these muscles *must* absorb and return some of the kinetic energy of the oscillating wing and virtual masses.

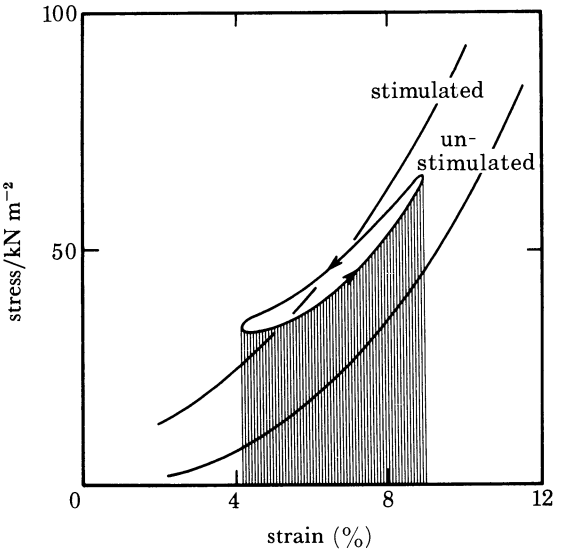

FIGURE 6. Typical stress/strain curve for intact fibrillar muscle of *Oryctes rhinoceros* under non-oscillatory (stimulated and unstimulated) and oscillatory (the loop) conditions. Adapted from Machin & Pringle (1959).

The characteristics of fibrillar muscle have often been reviewed (e.g. Pringle 1967, 1972, 1975). Figure 6 shows a typical stress/strain diagram for the intact fibrillar muscle of a coconut beetle *Oryctes rhinoceros*, adapted from Machin & Pringle (1959). The contractile activity of fibrillar muscle is maintained by a self-oscillatory mechanism that is under *mechanical*, not nervous, control. Indeed, an inertial load on the muscle is *essential* for oscillatory operation (the loop in figure 6); in the absence of an inertial load, or if it is highly damped, the muscle does not contract rhythmically. The muscle must always be under static tension, and it must also be stretched dynamically by the inertial load (the lower half of the loop) before it will contract (the upper half). The work done in stretching the muscle is given by the shaded area below the loop, and the work done during contraction is equal to this area plus the loop area. The *net* work per cycle is therefore equal to the area inside the loop, and is substantially smaller than the inertial energy absorbed and returned every cycle.

It is tempting to suggest that this inertial energy is stored and released by a passive elastic element, but the results of Machin & Pringle (1959) may not support this interpretation: the 'elastic' stiffness of the oscillating muscle, approximately given by the slope of the long axis of the loop, is somewhat less than the stiffness under non-oscillatory conditions (figure 6). We simply do not know the correct interpretation, and I shall refer loosely to an 'elastic' system for convenience.

Based on the contractile mechanics of fibrillar muscle, it seems logical to conclude that at least some of the inertial power of flight must be absorbed and released by the muscles. I shall initially assume that all of the inertial power is conserved, and the mean specific mechanical power output is then equal to the aerodynamic power $\overline{P^*_a}$. To convert this into the mean power per unit weight of *flight muscle*, $\overline{P^*_m}$, the ratio of flight muscle mass to body mass must be known. Greenewalt (1962) has collected data for insects and birds from the literature, and the ratio is about 14% for *Eristalis tenax*, *Apis mellifera* and several *Bombus* species. Therefore the mean mechanical power output per unit weight of flight muscle for DF01, HB01, BB04 and BB08 covers the small range of 17 to 19 W N^{-1}. If 14% is assumed for the other insects as well, the lowest value of $\overline{P^*_m}$ is likely to be 7 W N^{-1} for CF02.

Machin & Pringle (1959) measured a maximum mechanical power output $\overline{P^*_m}$ equal to 3 W N^{-1} for the intact fibrillar muscle of *Oryctes*, and 6 W N^{-1} for a bumble bee *Bombus terrestris*. They pointed out that these values are probably lower than those achieved during flight, because they could not mimic the special loading conditions produced by the natural wing articulation. Experiments on glycerol extracted fibrillar muscle yield even lower values (Jewell & Rüegg 1966; Pringle & Tregear 1969), and will not be discussed. It is interesting that the non-fibrillar flight muscle of the locust produces 8 W N^{-1} in level flight, and up to 17 W N^{-1} under extreme efforts (Weis-Fogh 1964). Weis-Fogh & Alexander (1977) estimate a maximum power output from striated muscle of about 26 W N^{-1}, and suggest that a similar value may apply to fibrillar muscle. All of these values refer to sustained aerobic power outputs, of course, and they indicate that the maximum for fibrillar muscle is no better than for striated. If the comments of Machin & Pringle (1959) are borne in mind, it should be reasonable to expect the fibrillar muscles to deliver say 20 W N^{-1} as required for *Eristalis* and the Hymenoptera, but perhaps no more. Thus their muscles are most likely to be operating near maximum power output just to satisfy the aerodynamic power demands of hovering, with little or no power available for inertial requirements. This directly contradicts the conclusion of Withers (1981), that inertial power is a substantial component in the power output of honey bees. He suggests that inertial power is about 1.8 times the aerodynamic power, and this would indicate that either $\overline{P^*_m}$ is much greater than 20 W N^{-1} or else the aerodynamic power is extremely low. Withers obtained his estimate by extrapolating metabolic data at different ambient air pressures according to aerodynamic relations that the data clearly did not obey, and I doubt whether this method can be as reliable as a straightforward mechanical analysis.

Based on the expected maximum mechanical power output, these estimates offer very strong evidence that 'elastic' storage of inertial energy is essential for insects with fibrillar muscles. We can also demonstrate that the muscles alone may not be capable of providing all the energy storage, so elastomers and cuticular elasticity might be involved as well. The maximum energy that can be stored 'elastically' in fibrillar muscle is about 0.13 J N^{-1} according to the calculations of Alexander & Bennet-Clark (1977). Only half of the muscle mass can be used to decelerate the wings over the second half of a given half-stroke, and the energy per unit weight of muscle involved is $(\overline{P^*_{acc}} - \overline{P^*_{ind}} - \overline{P^*_{pro}})/(0.07 \times 4n)$, or about 0.25 J N^{-1} for DF01, 0.15 for HB01 and BB04, and 0.20 for BB08. Based on the estimate of Alexander & Bennet-Clark, it thus appears that the muscles can store and release almost all of the inertial energy for HB01 and BB04, but only about 65% and 52% of it for BB08 and DF01. The remaining energy would have to be stored in other structures with a very high elastic efficiency if the mechanical power output of fibrillar muscle cannot substantially exceed about 20 W N^{-1}.

PHILOSOPHICAL TRANSACTIONS OF THE ROYAL SOCIETY B BIOLOGICAL SCIENCES

4.2.6. *Mechanochemical efficiency of flight muscle*

The values for mechanical power output can now be compared with measured metabolic rates to determine the efficiency of the fibrillar muscles. Weis-Fogh (1972, 1973) was hampered by the virtual absence of metabolic data for freely hovering insects, but fortunately the situation has changed since his studies. Modern interests in thermoregulation, ecology, and neural and biochemical control of flight metabolism have led to a wealth of new information, and several excellent reviews are available (Crabtree & Newsholme 1975; Kammer & Heinrich 1978; Casey 1981*c*; Candy & Kilby 1975; Heinrich 1981; for a review of the older work see Hocking 1953). Some of these modern results indicate that the metabolic rate in free flight can actually be double the value measured in tethered flight.

The flight metabolism of hovering insects has been reported many times in the last decade (Heinrich 1971, 1975; Heinrich & Casey 1973; Casey 1976*a*, *b*, 1980, 1981*b*; Bartholomew & Casey 1978; Withers 1981). Out of this selection, the oxygen consumption of honey bees and bumble bees is available for comparison with the insects in table 5. Heinrich (1975) measured a mean value of 80 ml O_2 g(body mass)$^{-1}$ h^{-1} for *Bombus* species during hovering, which is much greater than the value of 1.3 for 'resting' *B. vosnesenskii* (Kammer & Heinrich, 1974). Withers (1981) reported 94 ml O_2 g(body mass)$^{-1}$ h^{-1} for *Apis mellifera* in hovering, and a relatively high value of 12 during rest. In addition, Dr. F. S. Gilbert of the Department of Applied Biology, Cambridge has kindly let me use his unpublished measurement of 50 ml O_2 g(body mass)$^{-1}$ h^{-1} for *Eristalis tenax* in 'tethered' hovering: in his technique the insect had to support at least its own mass plus a small tether, which was only a small percentage of the body mass.

The metabolic rates during insect flight are often 50–100 times the resting level, and it is commonly assumed that the metabolic cost of physiological support systems is insignificant in flight. There is no reason to suspect that anaerobic metabolism is involved in sustained insect flight, so the metabolic power input can be estimated directly from the oxygen consumption using a standard conversion factor of about 20 J chemical energy per ml O_2. Neglecting the resting metabolism, the metabolic power input is therefore 45 W/N for *Bombus*, 53 W/N for *Apis*, and 28 W/N for *Eristalis*. The mechanochemical efficiency of the fibrillar muscles *assuming perfect elastic storage* is given by the mechanical power output ($= \overline{P^*_a}$) divided by the metabolic power input, and is 6% for *Bombus*, 5% for *Apis*, and 8% for *Eristalis*. Even if the relatively high resting metabolism of *Apis* is subtracted from the flight metabolism, its efficiency only increases to 6%.

These values are surprisingly low compared with the common expectation of 20–30%, based on measurements for vertebrate striated muscle (Dickinson 1929; Hill 1939, 1950; Cavagna *et al.* 1964; Tucker 1972; Bernstein *et al.* 1973; Pugh 1975; Thomas 1975; Margaria 1976). However, the mechanical power output of the fibrillar muscle, $\overline{P^*_m}$, would have to be much greater than 20 W N^{-1} to increase the efficiency significantly. Weis-Fogh (1972, 1973) estimated higher efficiencies for his insects, but the metabolic rates he used were much lower than those now obtained for hovering insects; for instance, the metabolic rates previously measured for *Apis* and *Eristalis* (Hocking 1953; Sotavalta & Laulajainen 1961) are about one-third of the values quoted above. Weis-Fogh assumed no elastic storage of inertial energy and even concluded that the resulting efficiencies could be too high, and that some insects must therefore possess an elastic system. This proof of the existence of elastic storage does not work

with the modern metabolic rates, though. The efficiency would be an acceptable 12% for *Apis*, 14% for *Bombus* and 29% for *Eristalis* if the muscles provided the power to accelerate the wings; the mechanical power output required for this would be 45–58 W N^{-1} of muscle, however, over twice the expected value.

The discussion so far has been limited to insects with fibrillar flight muscles, because suitable film sequences of hovering were not obtained for the Lepidoptera and Neuroptera in paper III. Casey (1981*a*) has examined the energetics of hovering sphinx moths using morphological and metabolic data from an earlier study (Bartholomew & Casey 1978) plus previously unpublished data. Sphinx (hawk) moths hover with a horizontal stroke plane, and are ideally suited for Weis-Fogh's (1973) mechanical analysis of hovering; indeed, he presented the kinematics of *Manduca sexta* to illustrate 'normal' hovering. Although Weis-Fogh estimated the mechanical power output for three sphingids, he did not compare the values with the metabolic rate in free hovering, available from Heinrich (1971). Casey thoroughly bridges this deficiency, offering mechanical estimates and metabolic data for some 28 sphingids.

Casey evaluated the mechanical power components by the method of Weis-Fogh (1973), except that the Rankine–Froude theory (Ellington 1978) instead of Weis-Fogh's 'correction' was used for the induced power. If there is perfect elastic storage of inertial energy, then the power output equals the total aerodynamic power, and Casey's values yield an average mechanochemical efficiency of 6% for the non-fibrillar flight muscle. If it is assumed instead that the muscles accelerate the wings without the aid of any elastic storage, the efficiency increases to 17%. By using the equations of §3 with his data for three *Manduca* specimens, my data on *M. sexta* (paper II), and some educated guesses, I also calculate very similar efficiencies. Because the value for no elastic storage is very close to the commonly expected 20–30%, Casey reasonably concluded that the mechanical power output must include a significant inertial power, and that substantial elastic saving is not indicated.

However, an efficiency argument leads to the same conclusion for *Eristalis* and the Hymenoptera, so a check on the specific power output of the flight muscles should prove informative. Although the proportion of flight muscle mass to body mass has not been reported for the sphingids that Casey considered, a value of 14% is available for the hummingbird hawk moth *Macroglossum stellatarum*, which has a body mass of 0.346 g (Greenewalt 1962). Casey showed that the specific aerodynamic power $\overline{P_a^*}$ is essentially constant for all sphingids regardless of body size, about 2.0 W N^{-1}. The specific inertial power, if no elastic storage is assumed, and the metabolic power input both increase with body mass, and his allometric equations yield values of 7.8 W N^{-1} and 53 W N^{-1} respectively for the mass of *Macroglossum*. The efficiency and mechanical power output of the flight muscles would therefore be 4% and 14 W N^{-1} of muscle for perfect elastic storage, and 18% and 70 W N^{-1} for no storage. If a maximum power output of about 20 W N^{-1} is tentatively accepted for the muscle, these results indicate that almost 90% of the inertial energy must be saved in elastic structures; the efficiency of the flight muscles would then be about 9%.

Bartholomew & Casey (1978) found that the ratio of thoracic mass to body mass decreases as body mass increases in the sphingids. If the flight muscle mass is a constant fraction of the thoracic mass, then the ratio of muscle mass to body mass should also decrease. *Macroglossum* is roughly the same size as the smallest sphingids investigated by Bartholomew & Casey, and their allometric equation indicates that the ratio of muscle mass to body mass may be only 10% for their largest sphingid. This would require 20 W N^{-1} of muscle for the aerodynamic

PHILOSOPHICAL TRANSACTIONS OF THE ROYAL SOCIETY B BIOLOGICAL SCIENCES

power alone, and suggests almost perfect elastic storage of inertial power. Thus the larger sphingids may have more effective elastic storage; this is another way of stating Casey's (1981*a*) conclusion that small sphingids 'waste' more inertial power.

These results are consistent with Weis-Fogh's (1972) report of a substantial elastic system in the cuticle of the thoracic box and in the wing ligaments of *Sphinx ligustri*. They contradict Casey's conclusion, though, and readers of his paper may wish to consider the following point. To support his conclusion that elastic storage is insignificant, Casey showed that the mechanical power output (calculated from the metabolic power input multiplied by an efficiency of 20%) minus the aerodynamic power output was roughly equal to his estimate of the inertial power output. However, the inertial power was calculated from the combined estimate of aerodynamic plus inertial power (if no elastic storage is assumed) minus the aerodynamic power. The net result of these manipulations only demonstrates that the combined estimate is about 20% of the metabolic power input, as indeed it is.

According to my analysis, either the efficiency of both fibrillar and non-fibrillar muscles is substantially lower than the commonly accepted 20–30%, or else the maximum mechanical power output is much greater than the expected 20–26 W N^{-1} of muscle. As with any theoretical estimates giving anomalous results, the analysis itself must obviously be suspected. I have therefore calculated the mechanical power components for a hovering hummingbird *Amazilia fimbriata* using data from Weis-Fogh (1972) and paper II. $\overline{P^*_{ind}}$ is 2.1 W N^{-1}, $\overline{P^*_{pro}}$ equals 0.3 W N^{-1}, and $\overline{P^*_{acc}}$ is 9.1 W N^{-1}. Weis-Fogh (1972) argued convincingly that little elastic storage is possible in vertebrate fliers, so the mechanical power output should be $\frac{1}{2}(\overline{P^*_{ind}}+\overline{P^*_{pro}}+\overline{P^*_{acc}})$. The metabolic power input is 24 W N^{-1} for hovering *Amazilia* (Berger & Hart 1972), and the flight muscles constitute 27% of the body mass (Greenewalt 1962). If no elastic storage is assumed, the mechanical power output is therefore 21 W N^{-1} of muscle, and the mechanochemical efficiency is 24%. Both of these estimates are quite acceptable for top quality vertebrate striated muscle, and thus provide some confidence in the analysis.

5. Conclusion

Although many of the results and conclusions of Weis-Fogh's (1973) comparative study have been disputed in this series of papers, this does not detract from his seminal work in any way. His paper was an excellent first approach to the aerodynamics of hovering flight, and was necessarily based on meagre and somewhat unreliable morphological and kinematic data. By combining the new data from papers II and III with the aerodynamic analyses of papers IV and V, this paper has re-examined the fundamental question posed by Weis-Fogh: to what extent do hovering animals rely on quasi-steady aerodynamics?

He concluded that animals using an inclined stroke plane must employ unsteady aerodynamics because the lift required of the wings exceeds that expected under quasi-steady conditions. The results for the hover-fly *Episyrphus balteatus* completely confirm his conclusion, revealing that a mean lift coefficient $\overline{C_L}$ of 4–5 is needed on the downstroke. Large downstroke lift coefficients are an unavoidable consequence of the inclined stroke plane, because the maximum profile drag possible on the downstroke imposes a limit to the horizontal thrust component, and thus the magnitude, of upstroke lift.

Visual estimates of the angles of attack indicate that the enhanced downstroke lift required for the hover-fly cannot be explained by aerodynamic mechanisms based only on translation

of the wings. Effective angles of attack for the hover-fly tend to be lower than the average for other hovering insects, and are smaller on the downstroke than the upstroke. Any lift mechanism based on the angles of attack of the translating wings would therefore predict less than average lift, with relatively more lift on the upstroke than the downstroke – predictions that clearly contradict the net force balance.

A rotational lift mechanism is postulated instead for the hover-fly, using the strong vorticity that must be shed during wing rotation at the ends of the wingbeat. Pronation is delayed and overlaps the beginning of the downstroke when the hover-fly uses an inclined stroke plane. As explained in paper IV, this increases the velocity of the leading edge with respect to the air during rotation, and should cause vortex shedding to be concentrated at the leading edge. The shed vorticity is likely to attach to the wing as a leading edge separation bubble during the subsequent downstroke, providing the circulation required for lift. This mechanism would create circulation before, and independently of, wing translation, and, like Weis-Fogh's fling mechanism, generates lift without the usual quasi-steady limitations. Unlike the fling mechanism, however, this mechanism of delayed pronation should work for a single wing in isolated rotation.

The hummingbirds and the vast majority of insects hover with a horizontal stroke plane, and support the body mass with equal lift on the downstroke and upstroke. Except for the few animals that use the fling mechanism, Weis-Fogh concluded that this group produces lift by the quasi-steady mechanism because estimates of $\overline{C_L}$ did not exceed $C_{L,max}$. The values were uncomfortably close, however, especially when the Wagner effect and the quality of the data available to Weis-Fogh are considered. Most of the insects in this study *could* generate the required lift from the quasi-steady mechanism, but two insects could not: the ladybird *Coccinella 7-punctata* and the crane-fly *Tipula obsoleta*. As with the hover-fly using an inclined stroke plane, alternative mechanisms based on the translational phase of the wingbeat are not consistent with the observed angles of attack for these two insects. Turning to possible rotational mechanisms, the enhanced lift of the ladybird can be explained by a near fling and partial fling if these mechanisms can generate even half of the circulation created by a complete fling. The crane-fly wings rotate in isolation, but flexion of the wing profile occurs halfway through rotation. This flexion could concentrate the vorticity shed during rotation at the leading edge, making it available for circulatory lift on the subsequent half-stroke: only about 25% of the vorticity likely to be shed during rotation need be recovered to generate sufficient lift for the crane-fly.

The kinematics of the honey bee, bumble bees, drone-fly, a hover-fly using a horizontal stroke plane, and a second crane-fly *T. paludosa* are basically the same as *T. obsoleta*, and we cannot accept the quasi-steady mechanism for them while rejecting it for the first crane-fly. All of these insects flex their wings in a similar manner, and the flex mechanism of lift generation may operate for them all. These results lead to the opposite conclusion from Weis-Fogh's, and indicate that most, if not all, hovering animals do not rely on quasi-steady aerodynamics, but use rotational lift mechanisms instead.

The new data and aerodynamic analyses do not alter significantly the mechanical power estimates of Weis-Fogh (1973) in general, although agreement between our results is fortuitous in some cases. The induced power requirement is only about 15% greater than the simple Rankine–Froude estimate for animals hovering with a horizontal stroke plane, but may be up to 60% higher for those using an inclined stroke plane. Profile power is of the same magnitude as induced power, giving aerodynamic efficiencies of 37–55%. The power needed to accelerate

the wing mass and virtual mass during the first half of a half-stroke is 1.4–5.9 times the aerodynamic power. Over the second half the net power requirement is negative; this indicates that the excess kinetic energy of the wing and virtual masses must be dissipated or stored elastically.

If perfect elastic storage is assumed, the mechanical power output would be 17–19 W N^{-1} of fibrillar flight muscle. This value is quite close to the 26 W N^{-1} estimated by Weis-Fogh & Alexander (1977) as the maximum power output for striated muscle, and they suggested that fibrillar muscle should be similar. Thus the fibrillar muscle may be operating near maximum power output just to satisfy the aerodynamic power demands, with little or no power available for inertial requirements. Considerable elastic storage of the kinetic energy of the wings would then be essential. This interpretation is consistent with the estimates of Alexander & Bennet-Clark (1977) on the maximum energy that could be stored elastically in fibrillar muscle, and the results of Machin & Pringle (1959) that fibrillar muscle *must* absorb and return the kinetic energy of an inertial load in order to maintain self-oscillation.

A maximum power output around 20 W N^{-1} yields mechanochemical efficiencies of only 5–8 % based on the metabolic rates of freely hovering insects, however. These values are much lower than the commonly accepted 20–30 %. Higher efficiencies would demand greater power output from the muscles, which would in turn require little elastic storage of the inertial power. Efficiencies of 12–29 % would result if there was no elastic storage, but the maximum power output from the fibrillar muscle would then be over twice the accepted value. Similar conclusions about efficiency and power output were also drawn for the non-fibrillar flight muscle of sphinx moths.

Neither the mechanochemical efficiency nor the maximum power output is actually known for fibrillar muscle. Substantial elastic storage in the muscle seems almost certain, though, and this indicates that low efficiencies and mechanical power outputs of about 20 W N^{-1} of muscle are quite likely. Using 20 W N^{-1} for the non-fibrillar muscle of sphinx moths results in an efficiency of 9 %, which is very close to the value of 11 % calculated by Weis-Fogh (1976) for locusts in level flight. Even though these low efficiencies for both types of insect flight muscle are somewhat disturbing, they are not necessarily worse than for vertebrate striated muscle: Heglund *et al.* (1982) have estimated comparable efficiencies for some birds and mammals in terrestrial locomotion.

I thank Dr F. S. Gilbert for permission to use his metabolic data on *Eristalis*, and Dr K. E. Machin and Dr T. M. Casey for stimulating discussions.

References

Abbott, B. C., Bigland, B. & Ritchie, J. M. 1952 The physiological cost of negative work. *J. Physiol., Lond* **117**, 380–390.

Alexander, R. McN. & Bennet-Clark, H. C. 1977 Storage of elastic strain energy in muscle and other tissues. *Nature, Lond.* **265**, 114–117.

Asmussen, E. 1952 Positive and negative muscular work. *Acta physiol. scand.* **28**, 364–382.

Bartholomew, G. A. & Casey, T. M. 1978 Oxygen consumption of moths during rest, pre-flight warm-up, and flight in relation to body size and wing morphology. *J. exp. Biol.* **76**, 11–25.

Berger, M. & Hart, J. S. 1972 Die Atmung beim Kolibri *Amazilia fimbriata* während des Schwirrfluges bei verschiedenen Umgebungstemperaturen. *J. comp. Physiol.* **81**, 363–380.

Bernstein, M. H., Thomas, S. P. & Schmidt-Nielsen, K. 1973 Power input during flight of the fish crow *Corvus ossifragus*. *J. exp. Biol.* **58**, 401–410.

PHILOSOPHICAL TRANSACTIONS OF THE ROYAL SOCIETY B BIOLOGICAL SCIENCES

Buchthal, F. & Weis-Fogh, T. 1956 Contribution of the sarcolemma to the force exerted by resting muscle of insects. *Acta physiol. scand.* **35**, 345–364.
Candy, D. J. & Kilby, B. A. (eds) 1975 *Insect biochemistry and function*. New York: Wiley.
Casey, T. M. 1976*a* Flight energetics of sphinx moths: power input during hovering flight. *J. exp. Biol.* **64**, 529–543.
Casey, T. M. 1976*b* Flight energetics of sphinx moths: heat production and heat loss in *Hyles lineata* during free flight. *J. exp. Biol.* **64**, 545–560.
Casey, T. M. 1980 Flight energetics and heat exchange of gypsy moths in relation to air temperature. *J. exp. Biol.* **88**, 133–145.
Casey, T. M. 1981*a* A comparison of mechanical and energetic estimates of flight cost for hovering sphinx moths. *J. exp. Biol.* **91**, 117–129.
Casey, T. M. 1981*b* Energetics and thermoregulation of *Malacosoma americanum* (Lepidoptera: Lasiocampidae) during hovering flight. *Physiol. Zool.* **54**, 362–371.
Casey, T. M. 1981*c* Insect flight energetics. In *Locomotion and energetics in arthropods* (ed. C. F. Herreid & C. R. Fourtner), pp. 419–452. New York: Plenum Press.
Cavagna, G. A., Saibene, F. P. & Margaria, R. 1964 Mechanical work in running. *J. appl. Physiol.* **19**, 249–256.
Crabtree, B. & Newsholme, E. A. 1975 Comparative aspects of fuel utilization and metabolism by muscle. In *Insect muscle* (ed. P. N. R. Usherwood), pp. 405–501. London: Academic Press.
Dickinson, S. 1929 The efficiency of bicycle pedalling, as affected by speed and load. *J. Physiol., Lond.* **67**, 242–255.
Ellington, C. P. 1975 Non-steady-state aerodynamics of the flight of *Encarsia formosa*. In *Swimming and flying in nature* (ed. T. Y. Wu, C. J. Brokaw & C. Brennen), vol. 2, pp. 783–796. New York: Plenum Press.
Ellington, C. P. 1978 The aerodynamics of normal hovering flight: three approaches. In *Comparative physiology – water, ions and fluid mechanics* (ed. K. Schmidt-Nielsen, L. Bolis & S. H. P. Maddrell), pp. 327–345. Cambridge University Press.
Ellington, C. P. 1980 Vortices and hovering flight. In *Instationäre Effekte an schwingenden Tierflügeln* (ed. W. Nachtigall), pp. 64–101. Wiesbaden: Franz Steiner.
Fage, A. & Johansen, F. C. 1927 On the flow of air behind an inclined flat plate of infinite span. *Rep. Memo. aeronaut. Res. Comm.* (*Coun.*) no. 1104.
Francis, R. H. & Cohen, J. 1933 The flow near a wing which starts suddenly from rest and then stalls. *Rep. Memo. aeronaut. Res. Comm.* (*Coun.*) no. 1561.
Greenewalt, C. H. 1962 Dimensional relationships for flying animals. *Smithson. misc. Collns* **144**(2), 1–46.
Heglund, N. C., Fedak, M. A., Taylor, C. R. & Cavagna, G. A. 1982 Energetics and mechanics of terrestrial locomotion. IV. Total mechanical energy changes as a function of speed and body size in birds and mammals. *J. exp. Biol.* **97**, 57–66.
Heinrich, B. 1971 Temperature regulation of the sphinx moth, *Manduca sexta*. I. Flight energetics and body temperature during free and tethered flight. *J. exp. Biol.* **54**, 141–152.
Heinrich, B. 1975 Thermoregulation in bumblebees. II. Energetics of warm-up and free-flight. *J. comp. Physiol.* **96**, 155–166.
Heinrich, B. (ed.) 1981 *Insect thermoregulation*. New York: Wiley.
Heinrich, B. & Casey, T. M. 1973 Metabolic rate and endothermy in sphinx moths. *J. comp. Physiol.* **82**, 195–206.
Hill, A. V. 1939 The mechanical efficiency of frog's muscle. *Proc. R. Soc. Lond.* B **127**, 434–451.
Hill, A. V. 1950 The dimensions of animals and their muscular dynamics. *Sci. Prog., Lond.* **38**, 209–230.
Hill, A. V. & Howarth, J. V. 1959 The reversal of chemical reactions in contracting muscle during an applied stretch. *Proc. R. Soc. Lond.* B **151**, 169–193.
Hocking, B. 1953 The instrinsic range and speed of flight of insects. *Trans. R. ent. Soc. Lond.* **104**, 223–345.
Hoerner, S. F. 1958 *Fluid-dynamic drag*. Midland Park, New Jersey: the author.
Huxley, A. F. & Simmons. R. M. 1971 Mechanical properties of the cross bridges of frog striated muscle. *J. Physiol., Lond.* **218**, 59*P*–60*P*.
Jensen, M. 1956 Biology and physics of locust flight. III. The aerodynamics of locust flight. *Phil. Trans. R. Soc. Lond.* B **239** 511–552.
Jewell, B. R. & Rüegg, J. C. 1966 Oscillatory contraction of insect fibrillar muscle after glycerol extraction. *Proc. R. Soc. Lond.* B **164**, 428–459.
Kammer, A. E. & Heinrich, B. 1974 Metabolic rates related to muscle activity in bumblebees. *J. exp. Biol.* **61**, 219–227.
Kammer, A. E. & Heinrich, B. 1978 Insect flight metabolism. *Adv. Insect Physiol.* **13**, 133–228.
Machin, K. E. & Pringle, J. W. S. 1959 The physiology of insect fibrillar muscle II. Mechanical properties of a beetle flight muscle. *Proc. R. Soc. Lond.* B **151**, 204–225.
Margaria, R. 1968 Positive and negative work performances and their efficiencies in human locomotion. *Int. Z. angew. Physiol.* **25**, 339–351.
Margaria, R. 1976 *Biomechanics and energetics of muscular exercise*. Oxford: Clarendon Press.
Maxworthy, T. 1979 Experiments on the Weis-Fogh mechanism of lift generation by insects in hovering flight. Part 1. Dynamics of the 'fling'. *J. Fluid Mech.* **93**, 47–63.
Maxworthy, T. 1981 The fluid dynamics of insect flight. *A. Rev. Fluid Mech.* **13**, 329–350.

PHILOSOPHICAL TRANSACTIONS OF THE ROYAL SOCIETY B BIOLOGICAL SCIENCES

Nachtigall, W. 1977 Die aerodynamische Polare des Tipula-Flügels und eine Einrichtung zur halbautomatischen Polarenaufnahme. In *The physiology of movement; biomechanics* (ed. W. Nachtigall), pp. 347–352. Stuttgart: Fischer.

Norberg, R.Å. 1975 Hovering flight of the dragonfly *Aeschna juncea* L., kinematics and aerodynamics. In *Swimming and flying in nature* (ed. T. Y. Wu, C. J. Brokaw & C. Brennen), vol. 2, pp. 763–781. New York: Plenum Press.

Norberg, U. M. 1975 Hovering flight of the pied flycatcher (*Ficedula hypoleuca*). In *Swimming and flying in nature* (ed. T. Y. Wu, C. J. Brokaw & C. Brennen), vol. 2, pp. 869–881. New York: Plenum Press.

Norberg, U. M. 1976 Aerodynamics of hovering flight in the long-eared bat *Plecotus auritus*. *J. exp. Biol.* **65**, 459–470.

Osborne, M. F. M. 1951 Aerodynamics of flapping flight with application to insects. *J. exp.Biol.* **28**, 221–245.

Pringle, J. W. S. 1967 The contractile mechanism of insect fibrillar muscle. *Prog. Biophys. molec. Biol.* **17**, 3–60.

Pringle, J. W. S. 1972 Arthropod muscle. In *The structure and function of muscle* (ed. G. H. Bourne), vol. 1, pp. 491–541. New York: Academic Press.

Pringle, J. W. S. 1975 Insect fibrillar muscle and the problem of contractility. In *Comparative physiology – functional aspects of structural materials* (ed. L. Bolis, S. H. P. Maddrell & K. Schmidt-Nielsen), pp. 139–152. Amsterdam: North-Holland.

Pringle, J. W. S. & Tregear, R. T. 1969 Mechanical properties of insect fibrillar muscle at large amplitudes of oscillation. *Proc. R. Soc. Lond.* B **174**, 33–50.

Pugh, L. G. C. E. 1974 The relation of oxygen intake and speed in competition cycling and comparative observations on the bicycle ergometer. *J. Physiol., Lond.* **241**, 795–808.

Rack, P. M. H. & Westbury, D. R. 1974 The short range stiffness of active mammalian muscle and its effect on mechanical properties. *J. Physiol., Lond.* **240**, 331–350.

Rayner, J. M. V. 1979 A new approach to animal flight mechanics. *J. exp. Biol.* **80**, 17–54.

Savage, S. B., Newman, B. G. & Wong, D. T.-M. 1979 The role of vortices and unsteady effects during the hovering flight of dragonflies. *J. exp. Biol.* **83**, 59–77.

Sotavalta, O. 1952 The essential factor regulating the wing-stroke frequency of insects in wing mutilation and loading experiments and in experiments at subatmospheric pressure. *Ann. Zool. Soc.* '*Vanamo*' **15**(2), 1–67.

Sotavalta, O. & Laulajainen, E. 1961 On the sugar consumption of the drone fly (*Eristalis tenax* L.) in flight experiments. *Suomalais.-ugr. Seur. Aikak.* (A. IV. Biol.) **53**, 1–25.

Thomas, S. P. 1975 Metabolism during flight in two species of bats, *Phyllostomus hastatus* and *Pteropus gouldii*. *J. exp. Biol.* **63**, 273–293.

Tucker, V. A. 1972 Metabolism during flight in the laughing gull, *Larus atricilla*. *Am. J. Physiol.* **222**, 237–245.

Weis-Fogh, T. 1959 Elasticity in arthropod locomotion: a neglected subject, illustrated by the wing system of insects. *XVth int. Congr. Zool.*, vol. 4, pp. 393–395.

Weis-Fogh, T. 1961 Power in flapping flight. In *The cell and the organism* (ed. J. A. Ramsay & V. B. Wigglesworth), pp. 283–300. Cambridge University Press.

Weis-Fogh, T. 1964 Biology and physics of locust flight. VIII. Lift and metabolic rate of flying locusts. *J. exp. Biol.* **41**, 257–271.

Weis-Fogh, T. 1965 Elasticity and wing movements in insects. *Proc. XIIth int. Congr. Ent.*, pp. 186–188.

Weis-Fogh, T. 1972 Energetics of hovering flight in hummingbirds and in Drosophila. *J. exp. Biol.* **56**, 79–104.

Weis-Fogh, T. 1973 Quick estimates of flight fitness in hovering animals, including novel mechanisms for lift production. *J. exp. Biol.* **59**, 169–230.

Weis-Fogh, T. 1976 Energetics and aerodynamics of flapping flight: a synthesis. In *Insect flight* (ed. R. C. Rainey), pp. 48–72. New York: Wiley.

Weis-Fogh, T. & Alexander, R. McN. 1977 The sustained power output from striated muscle. In *Scale effects in animal locomotion* (ed. T. J. Pedley). pp. 511–525. London: Academic Press.

Withers, P. C. 1981 The effects of ambient air pressure on oxygen consumption of resting and hovering honeybees. *J. comp. Physiol.* **141**, 433–437.

PHILOSOPHICAL TRANSACTIONS OF THE ROYAL SOCIETY B BIOLOGICAL SCIENCES